HAMILTONIAN FORMULATIONS AND SYMMETRIES IN ROD MECHANICS

DONALD J. DICHMANN*, YIWEI LI* , AND JOHN H. MADDOCKS*

1. Introduction. This article provides a survey of contemporary rod mechanics, including both dynamic and static theories. Much of what we discuss is regarded as classic material within the mechanics community, but the objective here is to provide a self-contained account accessible to workers interested in modelling DNA. We also describe a number of recent results and computations involving rod mechanics that have been obtained by our group at the University of Maryland. This work was largely motivated by applications to modelling DNA, but our approach reflects a background of research in continuum mechanics. In particular, we emphasize the role that Hamiltonian formulations and symmetries play in the effective computation of special solutions, conservation laws of dynamics and integrals of statics.

We begin in chapter 2 with an overview of the kinematics, balance laws and constitutive relations that collectively make up the director theory of rods, and which together determine the equations of motion. We then discuss some of the conservation laws which are implied by the evolution equations. In chapter 3 we describe various Hamiltonian formulations of the partial differential equations governing rod dynamics. In the case of a rod which is constrained to be inextensible and unshearable, the derivation of the Hamiltonian formulation is nonstandard and involves an approach we call the impetus-striction method. We conclude the chapter by delineating the Hamiltonian form of the invariants of motion. In chapter 4 we describe some Hamiltonian formulations of the ordinary differential equations governing the statics of rods. Following the same pattern as in chapter 3, we explicitly present Hamiltonians appropriate for both an extensible, shearable rod and for an inextensible, unshearable rod, and we then list the associated integrals. Finally in chapter 5 we discuss numerical continuation methods and describe the set of equilibria associated with what is now perhaps the prototypical problem for continuum models of DNA, namely a straight uniform rod, with circular cross-section, that is bent into a loop and then subjected to a prescribed twist (or linking difference).

In this article we have limited ourselves to a discussion of rod mechanics, and will not address the very interesting questions of how accurately a rod model actually describes DNA. In particular we do not discuss effects of solvents, nor the question of the statistical mechanics of rods. Nevertheless, the generality of the formulations we describe is somewhat suggestive

* Institute for Physical Science and Technology, and Department of Mathematics, University of Maryland, College Park, MD 20742. Research supported by AFOSR, NSF and ONR.

as a precursor to such analyses. In particular, the rod models we describe do account for natural curvature and twist, nonuniformity (as might arise from sequence dependence), anisotropy (e.g. unequal bending stiffnesses) and effects of self-contact. The Hamiltonian formulations lay bare the connections between conservation laws, integrals, special solutions, and the symmetries inherent to a straight, uniform rod, with circular cross-section. Moreover the numerical continuation methods we employ can be adapted so that the most symmetric, and by now comparatively standard case, can be exploited as an organizing center for computation of solutions in models where each of the symmetries is broken.

2. Classical Rod Mechanics.

2.1. Introduction. We adopt a relatively standard model based on the special Cosserat rod theory (cf. e.g. [1]). In a Cosserat rod theory, the concept of a rod is reduced to two components: a curve and a field of directors. The curve can be interpreted as describing the center line of the rod. The director field assigns to each point along the curve a set of three vectors (called directors), which provide a basis from which to describe the local bending, twisting, stretching and shearing of the rod. In the special Cosserat rod theory, the set of directors at each point is taken to be orthonormal, connoting the idea that the shape of each cross-section of the rod does not change significantly. In this general setting, the constitutive laws which relate the forces and moments within the rod to its bending, twisting, stretching and shearing need not be regarded as being determined by any assumed properties of a three-dimensional solid material such as linear elasticity. In the case of a model for DNA, the constitutive laws might instead be derived from experiments, or might be calculated from an atomistic simulation over a short segment.

The kinematics of a rod are first described in section 2.2. Next the force and moment balance laws are presented in section 2.3. The constitutive relations are discussed in section 2.4, with particular attention given to the modelling of an inextensible, unshearable elastic rod, i.e. an elastica. In section 2.5 we delineate the known conservation laws associated with rod mechanics, including a conservation law connected with translational symmetry which was found only recently. In section 2.6 we represent the kinematics of an elastica using Euler parameters, which, for computational purposes, have proved to be a very useful parametrization of the rotation group. The material presented in sections 2.2–2.4 is largely standard [1], some of the conservation laws described in section 2.5 were first presented in [29], and the material of section 2.6 is taken from [8].

2.2. Kinematics of rods. We begin by reviewing the director description of rod kinematics used in the special Cosserat theory. The dependent variables are a vector function $\boldsymbol{r}(s,t) \in \boldsymbol{R}^3$ and a right-handed orthonormal frame of directors $\boldsymbol{d}_k(s,t) \in \boldsymbol{R}^3$, $k = 1, 2, 3$. (Hereafter subscripts will be taken to run from 1 to 3, and repeated indices should be summed unless stated to the contrary.) The independent variables are two scalars, namely undeformed arc-length s, and time t. At each time t, the curve $\boldsymbol{r}(\cdot,t)$ can be interpreted as the configuration of the center line in a long, slender elastic body. The triad $\{\boldsymbol{d}_k\}$ can be interpreted as providing information concerning the orientation of the material cross-section of the rod. (See Figure 2.1.) The kinematics of the rod are encapsulated in the relations

$$\boldsymbol{r}' = \boldsymbol{v} \ , \tag{2.2.1}$$

$$\boldsymbol{d}_k' = \boldsymbol{u} \times \boldsymbol{d}_k \ , \tag{2.2.2}$$

$$\dot{\boldsymbol{d}}_k = \boldsymbol{\omega} \times \boldsymbol{d}_k \ . \tag{2.2.3}$$

Here $\boldsymbol{d}_k'$ denotes the partial derivative with respect to arc-length s, while $\dot{\boldsymbol{d}}_k$ denotes the partial derivative with respect to t, etc. The components $v_k \equiv \boldsymbol{v} \cdot \boldsymbol{d}_k$ of the vector $\boldsymbol{v}(s,t)$ with respect to the triad $\{\boldsymbol{d}_k\}$ are the strains associated with stretching and shear, the components $u_k \equiv \boldsymbol{u} \cdot \boldsymbol{d}_k$ of the (Darboux) vector $\boldsymbol{u}$ are the strains associated with bending and twist, and the components $\omega_k \equiv \boldsymbol{\omega} \cdot \boldsymbol{d}_k$ of the vector $\boldsymbol{\omega}(s,t)$ can be regarded as the director components of the angular velocity of the material cross-section at s when viewed as a rigid body. We will use u to denote the set of components (u_1, u_2, u_3), and similarly use v to denote (v_1, v_2, v_3).

Because v_k, u_k and ω_k are components with respect to a variable frame we obtain relations such as

$$\boldsymbol{\omega}' = \omega_k' \boldsymbol{d}_k + \boldsymbol{u} \times \boldsymbol{\omega} \ , \tag{2.2.4}$$

and

$$\boldsymbol{r}'' = \boldsymbol{v}' = v_k' \boldsymbol{d}_k + \boldsymbol{u} \times \boldsymbol{v} \ . \tag{2.2.5}$$

(By convention expressions such as v_k' involve the derivative of the kth component of $\boldsymbol{v}$ with respect to the triad $\{\boldsymbol{d}_j\}$, which is of course not the same as the kth component of $\boldsymbol{v}'$.) Equations (2.2.2), (2.2.3) and (2.2.4) in the identities

$$\frac{\partial^2}{\partial s \partial t} \boldsymbol{d}_k = \frac{\partial^2}{\partial t \partial s} \boldsymbol{d}_k \tag{2.2.6}$$

imply compatibility conditions such as

$$\dot{\boldsymbol{u}} = \omega_k' \boldsymbol{d}_k \ , \tag{2.2.7}$$

which place restrictions upon initial data in rod dynamics.

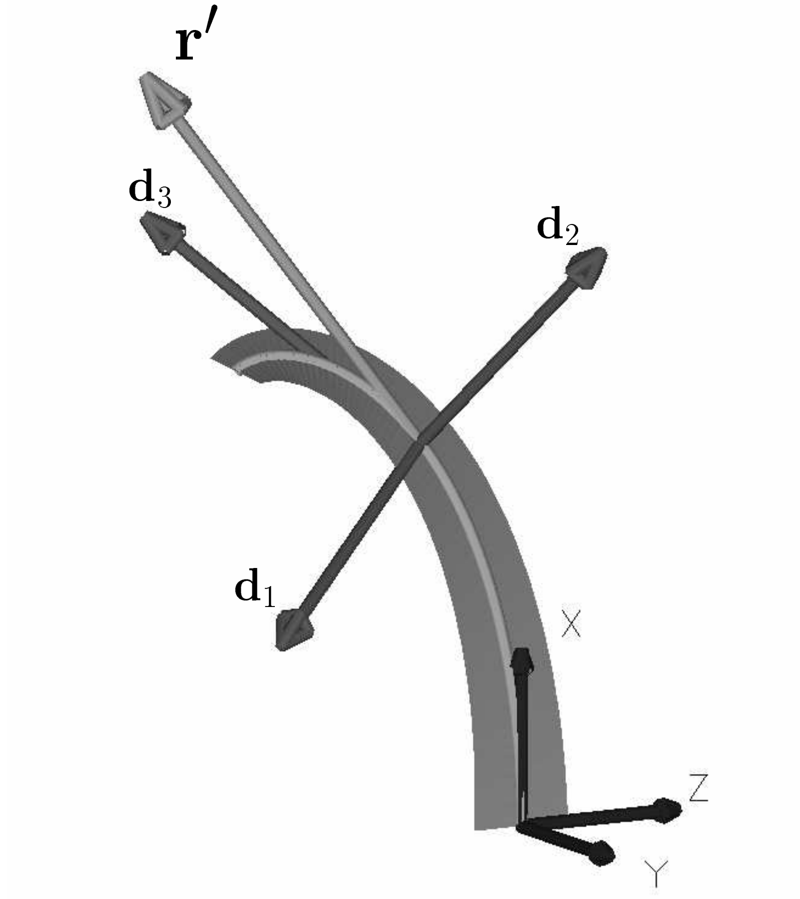

FIG. 2.1 *A ribbon representation of the configuration of a rod. The center curve is parameterized by undeformed arc-length s. The location of the material point at s is given by its position $\boldsymbol{r}(s)$ with respect to the origin. The directors $\boldsymbol{d}_1$, $\boldsymbol{d}_2$ and $\boldsymbol{d}_3$ describe the orientation of the cross-section of the rod at s, with $\boldsymbol{d}_1$ determining the ribbon. The components of $\mathbf{r}'$ with respect to the $\boldsymbol{d}_i$ basis determine the strains of shear and extension.*

2.3. Balance laws. The densities of linear and angular momentum are

$$\boldsymbol{p}(s,t) \equiv \rho(s)\dot{\boldsymbol{r}}, \tag{2.3.1}$$

$$\boldsymbol{\pi}(s,t) \equiv I_{ij}(s)\omega_i \boldsymbol{d}_j. \tag{2.3.2}$$

Here $\rho(s)$ is the mass per unit arc-length associated with the material cross-section at the point s, which is determined entirely by the reference configuration. The quantities $I_{ij}(s)$ are the components of the positive-definite inertia tensor of the material cross-section at s expressed with respect to the triad $\{\boldsymbol{d}_k\}$. In the special Cosserat rod model, it is assumed that these inertia coefficients are independent of the strains u_k and v_k. Thus the quantities $I_{ij}(s)$ are also completely determined by the reference configuration and will therefore be regarded as known. In particular the symmetry conditions

$$I_{ij} = I_{ji} \tag{2.3.3}$$

are valid. It is consistent to restrict to the case in which the cross-section is modelled as a lamina with principal axes of inertia $\boldsymbol{d}_1$ and $\boldsymbol{d}_2$, so that

$$I_{ij} = 0, \quad i \neq j, \qquad I_{33} = I_{11} + I_{22}. \tag{2.3.4}$$

Henceforth we make this assumption, and we write I_{jj} simply as I_j.

In a rod model, the stresses acting across each material cross-section are reduced to a net force $\boldsymbol{n}(s,t)$ and moment $\boldsymbol{m}(s,t)$ (of the material on the side s^+ acting on the material on the side s^- at the point $\boldsymbol{r}(s,t)$). In addition, the rod may be subject to an external distributed force $\boldsymbol{f}(s,t)$ and an external distributed moment $\boldsymbol{l}(s,t)$. Then balance of linear and angular momentum yield the equations

$$\dot{\boldsymbol{p}} = \boldsymbol{n}' + \boldsymbol{f}, \tag{2.3.5}$$

and

$$\dot{\boldsymbol{\pi}} = \boldsymbol{m}' + \boldsymbol{r}' \times \boldsymbol{n} + \boldsymbol{l}. \tag{2.3.6}$$

In most rod models the effects of external loads are neglected. In the modelling of DNA, two natural external loads to consider are self-interaction and the effects of a viscous solvent. We will not discuss viscous effects here. Self-interaction forces arise when the rod deforms in such a manner that points separated by large differences in arc-length become close to one another in space. The force in this case can be modelled in the general form

$$\boldsymbol{f}(s) = -\int M(s,\sigma)\frac{U'(|\boldsymbol{r}(s)-\boldsymbol{r}(\sigma)|)}{|\boldsymbol{r}(s)-\boldsymbol{r}(\sigma)|}\,[\boldsymbol{r}(s)-\boldsymbol{r}(\sigma)]\,d\sigma\ , \tag{2.3.7}$$

where U is a self-potential generating a central force between pairs of points along the rod, and M is a mollifier leading to finite total energy and corresponding, for example, to a nonzero radius of the rod. Here and henceforth, an integral is assumed to be taken over the length of the rod, unless otherwise specified. For the electrostatic Coulomb force, the potential U is proportional to $|\boldsymbol{r}(s) - \boldsymbol{r}(\sigma)|^{-1}$, but screening effects could well lead to more rapidly decaying potentials being appropriate. Notice, however, that in this context even the Coulomb potential is not long range, because (2.3.7) involves only a single integral, so that the total force does decay rapidly with distance. We take the corresponding external moment $\boldsymbol{l}(s)$ to be zero.

We shall be particularly interested in equilibrium solutions, for which the time derivatives in equations (2.3.5) and (2.3.6) must vanish, and a system of ordinary differential equations remains. The governing equations for an equilibrium are therefore

$$\boldsymbol{n}'(s) + \boldsymbol{f}(s) = \boldsymbol{0}, \tag{2.3.8}$$

and

$$\boldsymbol{m}'(s) + \boldsymbol{r}'(s) \times \boldsymbol{n}(s) + \boldsymbol{l}(s) = \boldsymbol{0}. \tag{2.3.9}$$

Note that in our derivation of a Hamiltonian form of equations (2.3.8) and (2.3.9), the arc-length s will play the role of 'time' in the evolution of an equilibrium solution. However it should be remembered that the physically appropriate supplementary conditions to (2.3.8) and (2.3.9) include boundary conditions at two values of s.

2.4. Constitutive relations. To complete the general formulation of rod dynamics, we must discuss the constitutive relations for both constrained and unconstrained motions. The nine equations contained in (2.2.3) and the three equations in each of (2.3.1), (2.3.5) and (2.3.6) together govern the time evolution of the motion of a rod. However these eighteen equations are not sufficient to determine the twenty-four dynamic variables, namely the components of the configuration $\boldsymbol{r}$, the directors $\{\boldsymbol{d}_k\}$ (i.e. an element of $SO(3)$), the strains $\boldsymbol{u}$ and $\boldsymbol{v}$, the linear momentum $\boldsymbol{p}$, the angular momentum $\boldsymbol{\pi}$, the force $\boldsymbol{n}$ and the moment $\boldsymbol{m}$. In the theory of elasticity it is postulated that the force $\boldsymbol{n}$ and moment $\boldsymbol{m}$ can be determined as functions of the current configuration of the rod. These constitutive relations are unlike the balance laws in that they are specific to the material of the rod. The manner in which $\boldsymbol{n}$ and $\boldsymbol{m}$ are determined depends upon whether the rod is materially unconstrained or constrained. Roughly speaking, the motion of a rod is said to be materially unconstrained if there are no restrictions upon the variables $\{v_k\}$ and $\{u_k\}$; otherwise, the motion is called constrained. This distinction must however be qualified, because most models of rod dynamics specify some conditions upon the strains, independent of the material properties, which are required for physically meaningful solutions. For example, one generally requires that

$$v_3 = \boldsymbol{v} \cdot \boldsymbol{d}_3 > 0 \tag{2.4.1}$$

be satisfied for all motions, so that a section of the rod of positive length cannot be compressed to zero length.

We consider only simple materials, for which $\boldsymbol{n}(s,t)$ and $\boldsymbol{m}(s,t)$ are functions of s, $\partial_s \boldsymbol{r}(s,t)$, and $\partial_s \boldsymbol{d}_k(s,t)$ only. It is known by the principle of frame indifference (cf. e.g. [1]) that $n_j \equiv \boldsymbol{n} \cdot \boldsymbol{d}_j$ and $m_j \equiv \boldsymbol{m} \cdot \boldsymbol{d}_j$ can be expressed as functions of the arc-length s and the six strains, $\{u_i\}$ and $\{v_i\}$. A case of special interest is the hyperelastic rod. A rod is said to be hyperelastic if there exists a scalar valued strain energy density function $W(v_i, u_i, s)$, dependent upon the six strains and arc-length, with the property that the components of stress satisfy the relations

$$n_j = W_{v_j}, \tag{2.4.2}$$

$$m_j = W_{u_j}. \tag{2.4.3}$$

In this article we will develop various Hamiltonian formulations assuming a general strain energy density function W. For concreteness, we will then focus upon the important special case, often called linearly elastic, where the strain energy is quadratic in the strains. In the case of an extensible shearable rod, the strain energy density then takes the form

$$W(\mathsf{u}-\hat{\mathsf{u}}, \mathsf{v}-\hat{\mathsf{v}}) = \tfrac{1}{2}K_j(u_j-\hat{u}_j)^2 + \tfrac{1}{2}A_j(v_j-\hat{v}_j)^2. \tag{2.4.4}$$

Here A_j, K_j, $\hat{v}_j$ and $\hat{u}_j$ are prescribed functions of s, possibly constant. In equation (2.4.4), the terms $\hat{\mathsf{u}} \equiv (\hat{u}_1, \hat{u}_2, \hat{u}_3)$ and $\hat{\mathsf{v}} \equiv (\hat{v}_1, \hat{v}_2, \hat{v}_3)$ describe the configuration of the unstressed rod. We will always assume that the unstressed state is unstretched and unsheared, so that $\hat{v}_1 = 0 = \hat{v}_2$ and $\hat{v}_3 = 1$. If in addition the unstressed state is also straight then $\hat{u}_j = 0$ for $j = 1, 2$, and if the unstressed state is untwisted $\hat{u}_3 = 0$. It follows from equations (2.4.2), (2.4.3) and (2.4.4) that the forces and moments in the linearly elastic case are given by

$$n_j = W_{v_j}(\mathsf{u}-\hat{\mathsf{u}}, \mathsf{v}-\hat{\mathsf{v}}) = A_j(v_j-\hat{v}_j)\ , \tag{2.4.5}$$

$$m_j = W_{u_j}(\mathsf{u}-\hat{\mathsf{u}}, \mathsf{v}-\hat{\mathsf{v}}) = K_j(u_j-\hat{u}_j)\ . \tag{2.4.6}$$

Models of rod mechanics often begin with the assumption that the rod is a solid object whose diameter is small compared to its length. This is the approach taken in the theory of Kirchhoff and Clebsch, which is described in [28], for example. If we adopt this point of view, and also assume that the material composing the rod is homogeneous and isotropic, then we can further interpret the elastic coefficients as $A_1 = A_2 = GA$, $A_3 = EA$, $K_j = EJ_j$ for $j = 1,\ 2$, $K_3 = GJ_3$, and $I_j = \rho J_j$, where A is the cross-sectional area of the rod, J_j is the geometric moment about the $\boldsymbol{d}_j$ axis (with $J_3 = J_1 + J_2$), E is Young's modulus, $G = E/[2(1+\nu)]$ is the shear modulus, and ν is Poisson's ratio. However, when modelling DNA as a rod, such an interpretation of the coefficients may not be appropriate.

One can also consider strain energies more general than that given by equation (2.4.4). In that case the quadratic function (2.4.4) may be viewed as the first terms in a Taylor series expansion of the strain energy, and so serve as an approximation to the exact strain energy. One can even consider a strain energy which is not convex as a function of the strains (cf. [18]), which is a model that might be appropriate for describing Z-form DNA.

We are particularly interested in the material constraints of inextensibility and unshearability, which are described by

$$\boldsymbol{r}_s = \boldsymbol{d}_3, \tag{2.4.7}$$

or equivalently

$$v_1 = 0 = v_2 \qquad \text{and} \qquad v_3 = 1. \tag{2.4.8}$$

Note that equation (2.4.8) automatically implies the inequality (2.4.1). For brevity equation (2.4.7) will henceforth be referred to as the inextensibility condition. It is stipulated that the constraint (2.4.7) holds for all possible forces and moments. In the model under consideration a constitutive equation is assumed only for the moments, in the form of equation (2.4.3). The force must instead be determined by the requirement that the constraint (2.4.7) be maintained. The rod will be assumed to be hyperelastic, and we will again begin with a general formulation of each Hamiltonian system, and then treat the specific example where the strain energy density is quadratic in the strains, namely

$$W(\mathsf{u} - \hat{\mathsf{u}}) = \tfrac{1}{2} K_j (u_j - \hat{u}_j)^2 \ . \tag{2.4.9}$$

The corresponding moment is given by equation (2.4.6).

2.5. Conservation laws. This section summarizes the conservation laws that are implied by the presence of continuous symmetry groups in the partial differential equations describing the dynamics of a rod. The material in this section is more fully discussed in [29].

For our purposes a conservation law means an expression of the form

$$D_t(s,t) = F_s(s,t), \tag{2.5.1}$$

where D, the density, and F, the flux, are each functions of the (scalar) independent variables s and t, and the (vector) dependent variable $\boldsymbol{y}$ and its derivatives:

$$D(s,t) = \tilde{D}(\boldsymbol{y}(s,t), \boldsymbol{y}'(s,t), \dot{\boldsymbol{y}}(s,t), s, t) \tag{2.5.2}$$

$$F(s,t) = \tilde{F}(\boldsymbol{y}(s,t), \boldsymbol{y}'(s,t), \dot{\boldsymbol{y}}(s,t), s, t) \tag{2.5.3}$$

One reason for our interest in conservation laws is that for boundary conditions such that the flux vanishes at the boundaries, each conservation law (2.5.1) can be integrated over the space variable s to yield an associated integral of motion

$$\frac{d}{dt}\int D(s)\,ds = 0. \tag{2.5.4}$$

On the other hand, in the context of statics the time derivative in equation (2.5.1) vanishes. Consequently, the flux is constant as a function of s along an equilibrium solution, and if the flux is nontrivial on static configurations, an integral of the ordinary differential equations governing equilibria is implied.

Conservation laws arise naturally in rod dynamics. It may be observed immediately that the balance of linear momentum (2.3.5) is in the form of a conservation law

$$\boldsymbol{p}_t = (\boldsymbol{n} + \boldsymbol{F})_s\ , \tag{2.5.5}$$

with density $\boldsymbol{p}$ and flux $\boldsymbol{n} + \boldsymbol{F}$, where

$$\boldsymbol{F} \equiv \int^s \boldsymbol{f}(\sigma)\,d\sigma \tag{2.5.6}$$

is the net external force on the rod up to the material point s. Moreover, we can use (2.3.1) and (2.3.5) to rewrite equation (2.3.6) in the conservation form

$$(\boldsymbol{\pi} + \boldsymbol{r} \times \boldsymbol{p})_t = (\boldsymbol{m} + \boldsymbol{r} \times \boldsymbol{n} + \boldsymbol{L})_s\ , \tag{2.5.7}$$

where

$$\boldsymbol{L} \equiv \int^s \{\boldsymbol{r}(\sigma) \times \boldsymbol{f}(\sigma) + \boldsymbol{l}(\sigma)\}\ d\sigma \tag{2.5.8}$$

is the net external moment on the rod up to material point s. Suppose that the net external force and moment on the rod vanish, as would occur in the case where external loads are due entirely to self-contact. Then for appropriate boundary conditions, such as the periodic ones pertinent for a closed loop, the total linear momentum $\int \boldsymbol{p}\,ds$ and total angular momentum $\int (\boldsymbol{\pi} + \boldsymbol{r} \times \boldsymbol{p})\,ds$ about a fixed origin are integrals of the motion, as could have been surmised at the outset. Conversely, equation (2.5.5) and (2.5.7) show that along an equilibrium solution the fluxes $\boldsymbol{n}(s) + \boldsymbol{F}(s)$ and $\boldsymbol{m}(s) + \boldsymbol{r}(s) \times \boldsymbol{n}(s) + \boldsymbol{L}(s)$ are constant.

Equations (2.5.5) and (2.5.7) are conservation laws independent of the constitutive relations. By contrast, the additional conservation laws that we discuss are associated with special properties of the constitutive relations, especially symmetries. In the important case where the rod is hyperelastic, one obtains the conservation law

$$(\tfrac{1}{2}\boldsymbol{p} \cdot \dot{\boldsymbol{r}} + \tfrac{1}{2}\boldsymbol{\pi} \cdot \boldsymbol{\omega} + W)_t = (\boldsymbol{m} \cdot \boldsymbol{\omega} + \boldsymbol{n} \cdot \dot{\boldsymbol{r}})_s. \tag{2.5.9}$$

In equation (2.5.9), W denotes $W(\mathsf{u}-\hat{\mathsf{u}}, \mathsf{v}-\hat{\mathsf{v}})$, and $\frac{1}{2}\boldsymbol{p}\cdot\dot{\boldsymbol{r}}+\frac{1}{2}\boldsymbol{\pi}\cdot\boldsymbol{\omega}+W$ is the energy density. Therefore if the flux $\boldsymbol{m}\cdot\boldsymbol{\omega}+\boldsymbol{n}\cdot\dot{\boldsymbol{r}}$ vanishes at the boundaries, as would occur if the ends are stationary or if periodic boundary conditions are imposed, then the total energy of the rod is conserved by the dynamics. In the case of statics, both $\dot{\boldsymbol{r}}$ and $\boldsymbol{\omega}$ vanish, so the resulting integral is trivial.

There is an additional conservation law for a rod that is both hyperelastic and uniform. The rod is said to be uniform if the coefficients ρ and I_{ij} are actually constants,

$$\rho' \equiv I'_{ij} \equiv 0, \tag{2.5.10}$$

and, in addition, the constitutive law (2.4.2) and (2.4.3) has no explicit dependence on the arc-length s. The associated symmetry is translation in arc-length. The following conservation law is then a consequence of the governing equations (2.3.5) and (2.3.6) that express balance of linear and angular momentum:

$$(\boldsymbol{\pi}\cdot\boldsymbol{u}+\boldsymbol{p}\cdot\boldsymbol{v})_t = \left(\boldsymbol{m}\cdot\boldsymbol{u}+\boldsymbol{n}\cdot\boldsymbol{v}-W+\tfrac{1}{2}\boldsymbol{\omega}\cdot\boldsymbol{\pi}+\tfrac{1}{2}\dot{\boldsymbol{r}}\cdot\boldsymbol{p}\right)_s . \tag{2.5.11}$$

It should be remarked that it is not assumed that $\hat{u}_j$ and $\hat{v}_j$ vanish, only that they are constant. Consequently the analysis presented here is valid for the dynamics of uniform hyperelastic rods whose unstressed state is helical.

The quantity

$$\int (\boldsymbol{\pi}\cdot\boldsymbol{u}+\boldsymbol{p}\cdot\boldsymbol{v})\, ds \tag{2.5.12}$$

is called the impulse, where it is again understood that the range of integration is the entire length of the rod. The impulse is actually a time-invariant quantity, i.e., a conserved quantity or integral of the dynamics, for systems with appropriate boundary conditions. For example in a finite closed loop of a rod, all the dependent variables must be periodic functions of s, and the impulse is therefore a conserved quantity. The impulse is not simply related to total linear momentum, which, for rod dynamics, is the integral generated by translational symmetry in space.

Notice that the flux appearing in the conservation law (2.5.11) is the Legendre transform of the density of total energy of the rod. In the special case of the statics of rods, the conservation law (2.5.11) implies that the Legendre transform of the strain energy density W, which is also the Hamiltonian for statics, is an integral.

We now drop the hypotheses that the rod is uniform and hyperelastic and instead assume that the rod is transversely isotropic. By transversely isotropic it is meant that the constitutive relations for the stresses and momenta are symmetric with respect to rotations about the director $\boldsymbol{d}_3$. In the special case of linear elasticity, transverse isotropy is equivalent to the conditions that $K_2 = K_1$, $I_2 = I_1$ and the unstressed configuration in not curved, so $\hat{u}_1 = \hat{u}_2 = 0$. As full isotropy, i.e., independence of the constitutive relation to arbitrary rotations of the basis $\{\boldsymbol{d}_i\}$, is not a pertinent concept in the context of rods, we shall henceforth allow the adjective transversely to stand by implication. Antman ([1], Theorem XIII.9.16) demonstrates that the hypothesis of isotropic elastic response is equivalent to the specialized constitutive relations

$$\boldsymbol{n} = N_1\boldsymbol{v} + N_2\boldsymbol{u} + N_3\boldsymbol{d}_3, \tag{2.5.13}$$

$$\boldsymbol{m} = M_1\boldsymbol{v} + M_2\boldsymbol{u} + M_3\boldsymbol{d}_3, \tag{2.5.14}$$

where the N_i, and M_i are each scalar functions of the six scalar arguments $|\boldsymbol{u}|$, $|\boldsymbol{v}|$, $\boldsymbol{u}\cdot\boldsymbol{v}$, u_3, v_3 and s. Isotropy of the dynamic properties of the rod follows when the expression (2.3.2) for the angular momentum is specialized to

$$\boldsymbol{\pi} \equiv I_1\boldsymbol{\omega} + (I_3 - I_1)\omega_3\boldsymbol{d}_3. \tag{2.5.15}$$

Here $\boldsymbol{d}_3$ is a principal axis of inertia with associated principal inertia $I_3(s)$, and the other two principal inertias both equal $I_1(s)$ (cf. (2.3.4) with $I_1 = I_2$). The general expression (2.3.1) for the linear momentum is already isotropic.

With the constitutive relations (2.5.13), (2.5.14) and (2.5.15), and the additional restriction

$$M_1(|\boldsymbol{u}|, \boldsymbol{u}\cdot\boldsymbol{v}, |\boldsymbol{v}|, u_3, v_3, s) \equiv N_2(|\boldsymbol{u}|, \boldsymbol{u}\cdot\boldsymbol{v}, |\boldsymbol{v}|, u_3, v_3, s), \tag{2.5.16}$$

the conservation law

$$(\boldsymbol{\pi}\cdot\boldsymbol{d}_3)_t = (\boldsymbol{m}\cdot\boldsymbol{d}_3)_s, \tag{2.5.17}$$

is a consequence of the angular momentum balance (2.3.6). In particular the derivation of (2.5.17) does not exploit the linear momentum balance (2.3.5) so the conservation law remains valid even for systems with external forces. The delimitation (2.5.16) is actually implied in the case of an isotropic hyperelastic rod where there is a strain energy function of the form $W(|\boldsymbol{u}|, \boldsymbol{u}\cdot\boldsymbol{v}, |\boldsymbol{v}|, u_3, v_3, s)$. Another plausible special case is $M_1 \equiv N_2 \equiv 0$.

The quantity

$$\int \boldsymbol{\pi}\cdot\boldsymbol{d}_3\, ds \tag{2.5.18}$$

will be called the (component of) isotropic angular momentum. The isotropic angular momentum is an integral of the motion for appropriate boundary conditions, for example the periodic conditions associated with a closed loop, as has already been observed by Simo *et al.* in [36]. On the other hand, in the case of statics, equation (2.5.17) implies that the component of moment $\boldsymbol{m}(s)\cdot\boldsymbol{d}_3(s)$ is an integral.

2.6. Representation of directors by Euler parameters. Thus far we have not specified any particular parametrization of the directors $\{\boldsymbol{d}_k\}$. For three-dimensional motion, a parametrization of the directors $\{\boldsymbol{d}_k\}$ is equivalent to selecting a representation for the group of orthogonal transformations $SO(3)$. In mechanics there are several common choices for such a representation. (Cf. e.g. [16].) Euler angles are often used because this representation uses the the minimum number of parameters, namely three. There are two significant drawbacks in using Euler angles. First, due to the topology of $SO(3)$ a set of three parameters cannot provide a global representation. In the case of Euler angles there is a direction in space at which the representation becomes singular. This singularity makes the study of dynamical systems a delicate matter, since the particular set of Euler angles must then be selected to avoid the singularity, or different charts must be used as the dynamics evolve. A second drawback in the use of Euler angles is the appearance of trigonometric functions, which can be computationally expensive.

Euler parameters provide a four-dimensional, global parametrization of $SO(3)$. In addition, only polynomial and rational functions arise in this representation. The difficulty with the Euler parameter representation is that the squares of the parameters must sum to one, which imposes a constraint upon the dynamics. A discussion of Euler parameters can be found, for example, in [5]. An elementary but self-contained description of the kinematics of Euler parameters, which appears in [8], is given below.

A set of Euler parameters is a quadruple of real numbers $\boldsymbol{q} = (q_1, q_2, q_3, q_4)^T$ (where T denotes the transpose) that satisfies the identity

$$\boldsymbol{q} \cdot \boldsymbol{q} = {q_1}^2 + {q_2}^2 + {q_3}^2 + q_4^2 = 1 \ . \tag{2.6.1}$$

The set of all quadruples satisfying (2.6.1) forms the unit sphere $\boldsymbol{S}^3$ in $\boldsymbol{R}^4$. A set of Euler parameters $\boldsymbol{q}$ is often called a unit quaternion, in connection with the algebra of quaternions [35]. In fact one reason that Euler parameters are so useful for the representation of $SO(3)$ is because the composition of two rotations may be expressed in an elegant manner which is closely related to the multiplication of quaternions.

By Euler's Theorem, the orientation of a frame of directors $\{\boldsymbol{d}_k\}$ with respect to a fixed frame $\{\boldsymbol{e}_k\}$ is described by a rotation through an angle Φ about an axis determined by a unit vector $\boldsymbol{k} = k_j \boldsymbol{e}_j$. The Euler parameters (q_1, q_2, q_3, q_4) are defined in terms of $\boldsymbol{k}$ and Φ by

$$q_j = k_j \sin(\Phi/2) \ , \qquad \text{for } j = 1, 2, 3 \tag{2.6.2}$$

and

$$q_4 = \cos(\Phi/2) \ . \tag{2.6.3}$$

Euler parameters have the feature that if $\boldsymbol{q}$ corresponds to the pair $(\boldsymbol{k}, \Phi)$, then $-\boldsymbol{q}$ corresponds to the pair $(\boldsymbol{k}, \Phi + 2\pi)$ which represents a coterminal rotation. Thus there is a two-to-one correspondence between Euler parameters and rotations. To obtain a Hamiltonian system describing rod dynamics, we express the directors in terms of Euler parameters as

$$\boldsymbol{d}_1 = \frac{1}{|\boldsymbol{q}|^2} \begin{pmatrix} q_1^2 - q_2^2 - q_3^2 + q_4^2 \\ 2(q_1 q_2 + q_3 q_4) \\ 2(q_1 q_3 - q_2 q_4) \end{pmatrix}, \tag{2.6.4}$$

$$\boldsymbol{d}_2 = \frac{1}{|\boldsymbol{q}|^2} \begin{pmatrix} 2(q_1 q_2 - q_3 q_4) \\ -q_1^2 + q_2^2 - q_3^2 + q_4^2 \\ 2(q_2 q_3 + q_1 q_4) \end{pmatrix}, \tag{2.6.5}$$

$$\boldsymbol{d}_3 = \frac{1}{|\boldsymbol{q}|^2} \begin{pmatrix} 2(q_1 q_3 + q_2 q_4) \\ 2(q_2 q_3 - q_1 q_4) \\ -q_1^2 - q_2^2 + q_3^2 + q_4^2 \end{pmatrix}. \tag{2.6.6}$$

The factor of $1/|\boldsymbol{q}|^2$ appearing in equations (2.6.4) – (2.6.6) is not generally used in this representation. We introduce the term in order to make the directors explicitly orthonormal. By doing so, we introduce a scaling symmetry into the Hamiltonian system whereby $\boldsymbol{q}$ may be replaced by $\epsilon\boldsymbol{q}$ without altering the dynamics. The advantage of this scaling is discussed further in section 3.3.

The strains u_j and the angular velocities ω_j appearing in equations (2.2.2) and (2.2.3) are given in terms of the Euler parameters by

$$u_j = \frac{2}{|\boldsymbol{q}|^2} \boldsymbol{B}_j \boldsymbol{q} \cdot \boldsymbol{q}_s \tag{2.6.7}$$

and

$$\omega_j = \frac{2}{|\boldsymbol{q}|^2} \boldsymbol{B}_j \boldsymbol{q} \cdot \boldsymbol{q}_t \ , \tag{2.6.8}$$

where $\boldsymbol{B}_1\boldsymbol{q}$, $\boldsymbol{B}_2\boldsymbol{q}$ and $\boldsymbol{B}_3\boldsymbol{q}$ are vectors given by

$$\boldsymbol{B}_1\boldsymbol{q} = \begin{pmatrix} q_4, & q_3, & -q_2, & -q_1 \end{pmatrix}^T , \tag{2.6.9}$$

$$\boldsymbol{B}_2\boldsymbol{q} = \begin{pmatrix} -q_3, & q_4, & q_1, & -q_2 \end{pmatrix}^T , \tag{2.6.10}$$

$$\boldsymbol{B}_3\boldsymbol{q} = \begin{pmatrix} q_2, & -q_1, & q_4, & -q_3 \end{pmatrix}^T . \tag{2.6.11}$$

The vectors $\{\boldsymbol{B}_j\boldsymbol{q}\}$, together with $\boldsymbol{q}$, form an orthonormal basis for $\boldsymbol{R}^4$. Moreover $\boldsymbol{B}_j\boldsymbol{q}$ is linear in the Euler parameters, which simplifies computations. The vector $\boldsymbol{B}_k\boldsymbol{q}$ can be used to describe the rotation about the $\boldsymbol{d}_k$ axis in terms of Euler parameters. There is a related set of vectors $\{\boldsymbol{B}_k^o\boldsymbol{q}\}$ which describe rotations about the $\boldsymbol{e}_k$ axes,

$$\boldsymbol{B}_1^o\boldsymbol{q} = \begin{pmatrix} q_4, & -q_3, & q_2, & -q_1 \end{pmatrix}^T , \tag{2.6.12}$$

$$\boldsymbol{B}_2^o\boldsymbol{q} = \begin{pmatrix} q_3, & q_4, & -q_1, & -q_2 \end{pmatrix}^T , \tag{2.6.13}$$

$$\boldsymbol{B}_3^o\boldsymbol{q} = \begin{pmatrix} -q_2, & q_1, & q_4, & -q_3 \end{pmatrix}^T . \tag{2.6.14}$$

To facilitate the writing of the Hamiltonian equations of motion, we define the matrices

$$\boldsymbol{D}_k[\boldsymbol{q}] \equiv \left(\frac{\partial \boldsymbol{d}_k}{\partial \boldsymbol{q}}\right)^T , \tag{2.6.15}$$

and note that these matrices can be expressed in terms of the bases $\{\boldsymbol{B}_j\boldsymbol{q}\}$ and $\{\boldsymbol{d}_j(\boldsymbol{q})\}$ as

$$\boldsymbol{D}_k[\boldsymbol{q}] = \frac{2}{|\boldsymbol{q}|^2}\epsilon_{ijk}\boldsymbol{B}_j\boldsymbol{q}\otimes\boldsymbol{d}_i = \frac{2}{|\boldsymbol{q}|^2}\boldsymbol{B}_j\boldsymbol{q}\otimes(\boldsymbol{d}_j\times\boldsymbol{d}_k) , \tag{2.6.16}$$

where ϵ_{ijk} is the permutation tensor and $\otimes$ denotes the outer product. Geometrically, a change in $\boldsymbol{q}$ by $\epsilon\boldsymbol{B}_k\boldsymbol{q}$ can be interpreted as the instantaneous rotation about the $\boldsymbol{d}_k$ axis through an angle 2ϵ, which does not change $\boldsymbol{d}_k$ itself.

The kinetic energy can be expressed in terms of the Euler parameters as

$$T(\boldsymbol{r},\boldsymbol{q}) = \int \tfrac{1}{2}\left\{\rho|\boldsymbol{r}_t|^2 + I_j\omega_j^2\right\} ds , \tag{2.6.17}$$

where ω_j is given by equation (2.6.8). Similarly the potential energy becomes

$$V[\boldsymbol{q}] = \int W(\mathsf{u}-\hat{\mathsf{u}},\mathsf{v}-\hat{\mathsf{v}})\, ds , \tag{2.6.18}$$

where u is given by equation (2.6.7).

In statics, it transpires that there is more freedom in the scaling of Euler parameters and the factor $1/|\boldsymbol{q}|^2$ appearing in equations (2.6.4) – (2.6.6) can be replaced with $1/|\boldsymbol{q}|^\beta$ for any β and a symmetry in the Hamiltonian system is still obtained. It is therefore convenient to employ the standard formulation with $\beta = 0$, namely

$$\boldsymbol{d}_1 = \begin{pmatrix} q_1^2 - q_2^2 - q_3^2 + q_4^2 \\ 2(q_1q_2 + q_3q_4) \\ 2(q_1q_3 - q_2q_4) \end{pmatrix} , \tag{2.6.19}$$

$$\boldsymbol{d}_2 = \begin{pmatrix} 2(q_1q_2 - q_3q_4) \\ -q_1^2 + q_2^2 - q_3^2 + q_4^2 \\ 2(q_2q_3 + q_1q_4) \end{pmatrix} , \tag{2.6.20}$$

$$\boldsymbol{d}_3 = \begin{pmatrix} 2(q_1q_3 + q_2q_4) \\ 2(q_2q_3 - q_1q_4) \\ -q_1^2 - q_2^2 + q_3^2 + q_4^2 \end{pmatrix} . \tag{2.6.21}$$

The strains u_j are still given in terms of the Euler parameters by

$$u_j = \frac{2}{|\boldsymbol{q}|^2}\boldsymbol{B}_j\boldsymbol{q}\cdot\boldsymbol{q}_s \ , \tag{2.6.22}$$

but this scaling, the matrices $\boldsymbol{D}_k[\boldsymbol{q}]$ take a slightly different form, namely

$$\boldsymbol{D}_k[\boldsymbol{q}] = \frac{2}{|\boldsymbol{q}|^2}\epsilon_{ijk}\boldsymbol{B}_j\boldsymbol{q}\otimes\boldsymbol{d}_i + \frac{2}{|\boldsymbol{q}|^2}\boldsymbol{q}\otimes\boldsymbol{d}_k \ . \tag{2.6.23}$$

In statics it is the potential energy density, rather than the total potential energy, which arises in a variational formulation. In this case the potential energy density of the rod is

$$W(\mathsf{u}-\hat{\mathsf{u}}, \mathsf{v}-\hat{\mathsf{v}}) \ , \tag{2.6.24}$$

where u is given by equation (2.6.22).

3. Hamiltonian Formulations of Dynamics.

3.1. Introduction. In this chapter we describe various Hamiltonian formulations of rod dynamics, for both unconstrained and constrained motion. In each instance, the Hamiltonian system is a set of partial differential equations which can be expressed compactly as

$$\boldsymbol{z}_t = \boldsymbol{J}\,\delta H(\boldsymbol{z}) \ . \tag{3.1.1}$$

In equation (3.1.1), $\boldsymbol{z}(s,t)$ is a vector with fourteen components consisting of $\boldsymbol{r}(s,t)$, $\boldsymbol{q}(s,t)$ and their conjugate variables, and $\boldsymbol{J}$ is the 14-by-14 skew symmetric matrix given by

$$\boldsymbol{J} = \begin{pmatrix} \mathbf{0} & \mathbf{1} \\ -\mathbf{1} & \mathbf{0} \end{pmatrix} , \tag{3.1.2}$$

where $\mathbf{0}$ is the 7-by-7 zero matrix, and $\mathbf{1}$ is the 7-by-7 identity matrix. The Hamiltonian H is defined as an integral of the energy density over the length of the rod, and δH denotes its variational derivative.

Hamiltonian formulations are valuable for both analytical and computational reasons. The dynamics are first-order in time, which can simplify both analysis and numerics. There is a very simple relationship, via Noether's Theorem, between symmetries and integrals of motion. The existence of integrals strongly affects the qualitative behavior of Hamiltonian systems. In addition, through a careful choice of numerical integration scheme one can preserve a finite number of integrals of motion in order to better reflect the exact solution.

In the study of rod dynamics, unconstrained constitutive relations are much more tractable than constrained constitutive relations. The first Hamiltonian formulation of unconstrained rods of which we are aware is by Simo *et al.* [36]. Simo and Vu-Quoc [37] have also employed Euler parameters in a numerical model of rod dynamics.

The dynamics of constrained rods are more complicated. In the limit of unshearability and inextensibility, the speed of shear and compression waves becomes infinite. In this limit the shear and extensive forces also become basic unknowns, replacing the respective strains. Moreover the equations governing the forces are elliptic boundary value problems, so one obtains hyperbolic equations coupled to elliptic ones. (This is familiar in the context of incompressible fluid flow where there is an elliptic boundary value problem for the pressure field.) The first place we are aware that this observation was applied within the context of rods is Caflisch & Maddocks [6], which proved analytic results regarding existence of solutions for the planar case. Falk and Xu [15] then built a related planar numerical scheme, and Coleman and Xu [7] studied planar travelling waves both analytically and numerically. All of these works involved constrained Lagrangian dynamics. In his thesis Dichmann [8] showed how to obtain unconstrained Hamiltonian formulations of constrained Lagrangian systems, employing a novel approach we call the impetus-striction method, with the main example being constrained rods. The planar version of this Hamiltonian formulation for an inextensible, unshearable rod was used to produce an analytic proof of the stability of travelling waves [9]. The full three-dimensional equations are derived in [8]. The planar case has been implemented numerically, and the three-dimensional version of the code is in preparation [10].

There are two related works of which we are aware that consider rod dynamics in the context of DNA modelling. Schlick *et al.* [34] (and references therein) have developed an approach in which the centerline of the rod is described by B-splines, and the effects of twist are captured using a prescribed linking difference and the relation $\mathrm{Lk} = \mathrm{Tw} + \mathrm{Wr}$. Time evolution is introduced by allowing the spline points to evolve according to a certain molecular dynamics model. While this model is perfectly viable when used as part of a Monte-Carlo procedure for the minimization of static energy, there are two drawbacks in its interpretation as a true dynamic evolution. First, the relation between the dynamics assigned to the spline points and the actual dynamics of the rod are unclear. Second, the use of the Lk = Tw + Wr formula to eliminate the local twist from the total energy assumes that the local twist is constant, which is the case only if the twist is equilibriated at all times, and the rod is isotropic. In particular there can be no curvature in the unstressed state, and the two bending stiffnesses must be equal. Even in the case of an isotropic uniform rod, the ensuing dynamics are quasi-static in the twist evolution. In another work Klapper and Tabor [21] make an assumption that is in some sense complementary to that of [34]. Klapper and Tabor examine full twist dynamics, but they make a different simplifying assumption that in a certain sense equilibriates the two bending moments, and gives quasi-static evolution in bending while having dynamic effects in twist. A similar approximation was made by Beliaev and Illichev [3] in the case of planar dynamics where the approximation is certainly consistent, but a justification of the approximation in the case of three dimensional dynamics is less clear. The parameter regimes and circumstances in which the approximations made in [34] and [21] would yield reasonably accurate models of rod dynamics is an interesting, but open area of investigation.

For simplicity we assume in this chapter that there are no external loads. In particular we neglect effects of self-contact. In section 3.2 we present a Hamiltonian formulation for the three-dimensional dynamics of an extensible, shearable rod. Then in section 3.3 we describe a Hamiltonian formulation for the dynamics of an elastica. In each case we begin with the formulation for a general strain energy density, then specialize to the case of linear elasticity. Finally in section 3.4 we delineate the associated invariants of motion for both Hamiltonian systems, including those listed in section 2.5 as well as two families of invariants which are specific to the Hamiltonian formulations.

3.2. Hamiltonian formulation of the dynamics of an extensible, shearable rod. Let us first consider a general strain energy of the form $W(\mathsf{u}-\hat{\mathsf{u}},\mathsf{v}-\hat{\mathsf{v}})$, where $\mathsf{u}=(u_1,u_2,u_3)$ is given by (2.6.7). The Hamiltonian, which is the total energy, is given by

$$\begin{aligned} H(\boldsymbol{r},\boldsymbol{q},\boldsymbol{p},\boldsymbol{\zeta}) &= \int \left\{ \tfrac{1}{2}\rho^{-1}|\boldsymbol{p}|^2 + \tfrac{1}{2} I_j^{-1}\left(\tfrac{1}{2}\boldsymbol{B}_j\boldsymbol{q}\cdot\boldsymbol{\zeta}\right)^2 \right\} ds \\ &\quad + \int W(\mathsf{u}-\hat{\mathsf{u}},\mathsf{v}-\hat{\mathsf{v}})\, ds\ , \end{aligned} \tag{3.2.1}$$

where $\boldsymbol{p}$ is the linear momentum (2.3.1) which is conjugate to the position $\boldsymbol{r}$, and $\boldsymbol{\zeta}$ is the momentum variable conjugate to $\boldsymbol{q}$, given by

$$\boldsymbol{\zeta} = I_j\left(\frac{2\boldsymbol{B}_j\boldsymbol{q}\cdot\boldsymbol{q}_t}{|\boldsymbol{q}|^2}\right)\frac{2\boldsymbol{B}_j\boldsymbol{q}}{|\boldsymbol{q}|^2} + \nu\boldsymbol{q}\ . \tag{3.2.2}$$

In equation (3.2.2), ν is a Lagrange multiplier associated with the constraint (2.6.1). Here, and in the subsequent Hamiltonian formulations, we use

Greek letters to represent conjugate variables that have no classic physical interpretation.

To solve equation (3.2.2) for $\boldsymbol{q}_t$ and ν, one must use the constraint (2.6.1) together with the orthogonality of the basis $\{\boldsymbol{q}, \boldsymbol{B}_j\boldsymbol{q}\}$ in order to obtain

$$\boldsymbol{q}_t = I_j^{-1}\left(\tfrac{1}{2}\boldsymbol{B}_j\boldsymbol{q}\cdot\boldsymbol{\zeta}\right)\left(\tfrac{1}{2}\boldsymbol{B}_j\boldsymbol{q}\right) \tag{3.2.3}$$

and

$$\nu = \frac{\boldsymbol{q}\cdot\boldsymbol{\zeta}}{|\boldsymbol{q}|^2}\ . \tag{3.2.4}$$

It is necessary to invoke the constraint (2.6.1) in order to solve (3.3.3) for $\boldsymbol{q}_t$, for otherwise the component $\boldsymbol{q}\cdot\boldsymbol{q}_t$ is indeterminate. This is a special case of a general theory developed by Dirac [11], which constructs Hamiltonian formulations of Lagrangian systems that are not strictly convex in the velocities.

It follows from equation (3.2.1) that the Hamiltonian dynamics are given by

$$\boldsymbol{r}_t = \frac{\delta H}{\delta\boldsymbol{\chi}} = \rho^{-1}\boldsymbol{p}\ , \tag{3.2.5}$$

$$\boldsymbol{q}_t = \frac{\delta H}{\delta\boldsymbol{\zeta}} = I_j^{-1}\left(\tfrac{1}{2}\boldsymbol{B}_j\boldsymbol{q}\cdot\boldsymbol{\zeta}\right)\tfrac{1}{2}\boldsymbol{B}_j\boldsymbol{q}\ , \tag{3.2.6}$$

$$\boldsymbol{p}_t = -\frac{\delta H}{\delta\boldsymbol{r}} = \left(W_{v_j}\boldsymbol{d}_j\right)_s\ , \tag{3.2.7}$$

$$\begin{aligned}\boldsymbol{\zeta}_t = -\frac{\delta H}{\delta\boldsymbol{q}} &= I_j^{-1}\left(\tfrac{1}{2}\boldsymbol{B}_j\boldsymbol{q}\cdot\boldsymbol{\zeta}\right)\tfrac{1}{2}\boldsymbol{B}_j\boldsymbol{\zeta}\\ &\quad+W_{u_j}\left(\frac{2\boldsymbol{B}_j\boldsymbol{q}_s}{|\boldsymbol{q}|^2}+\frac{2\boldsymbol{B}_j\boldsymbol{q}\cdot\boldsymbol{q}_s}{|\boldsymbol{q}|^2}\frac{2\boldsymbol{q}}{|\boldsymbol{q}|^2}\right)\\ &\quad+\left(W_{u_j}\frac{2\boldsymbol{B}_j\boldsymbol{q}}{|\boldsymbol{q}|^2}\right)_s - W_{v_j}\boldsymbol{D}_j\,\boldsymbol{r}_s\ ,\end{aligned} \tag{3.2.8}$$

where W is a function of $\mathsf{u}-\hat{\mathsf{u}}$ and $\mathsf{v}-\hat{\mathsf{v}}$, the matrices $\boldsymbol{B}_j$ and $\boldsymbol{D}_j$ are defined by equations (2.6.9) – (2.6.11) and (2.6.16), and there is an implied summation on the j index. In the special case of linear elasticity, the Hamiltonian dynamics can be simplified using equations (2.4.5) and (2.4.6).

3.3. Hamiltonian formulation of the dynamics of an elastica. We now turn our attention to the three-dimensional motion of an inextensible and unshearable rod (i.e., an elastica) in terms of Euler parameters. The details of the derivation of this Hamiltonian system of equations can be found in [8], Chapter 6.

For a general strain energy of the form $W(\mathsf{u}-\hat{\mathsf{u}})$, where $\mathsf{u}=(u_1,u_2,u_3)$ is given by (2.6.7), the Hamiltonian is

$$
\begin{aligned}
H(\boldsymbol{r},\boldsymbol{q},\boldsymbol{\chi},\boldsymbol{\gamma}) &= \int \left\{ \tfrac{1}{2}\rho^{-1}|\boldsymbol{\chi}+\tilde{\boldsymbol{\Lambda}}_s|^2 + \tfrac{1}{2}I_j^{-1}\left(\tfrac{1}{2}\boldsymbol{B}_j\boldsymbol{q}\cdot\boldsymbol{\gamma}+\epsilon_{ij3}\boldsymbol{d}_i\cdot\tilde{\boldsymbol{\Lambda}}\right)^2\right\} ds \\
&\quad + \int W(\mathsf{u}-\hat{\mathsf{u}})\, ds \;. \qquad (3.3.1)
\end{aligned}
$$

In equation (3.3.1), $\boldsymbol{\chi}$ is the momentum variable conjugate to the position $\boldsymbol{r}$ defined by

$$
\boldsymbol{\chi} = \rho\boldsymbol{r}_t - \boldsymbol{\Lambda}_s \;, \qquad (3.3.2)
$$

while $\boldsymbol{\gamma}$ is the momentum variable conjugate to $\boldsymbol{q}$ and is given by

$$
\boldsymbol{\gamma} = I_j\left(\frac{2\boldsymbol{B}_j\boldsymbol{q}\cdot\boldsymbol{q}_t}{|\boldsymbol{q}|^2}\right)\frac{2\boldsymbol{B}_j\boldsymbol{q}}{|\boldsymbol{q}|^2} - \boldsymbol{D}_3[\boldsymbol{q}]\boldsymbol{\Lambda} + \nu\boldsymbol{q} \;. \qquad (3.3.3)
$$

In equations (3.3.2) and (3.3.3), ν has the same meaning as in section 3.2, and $\boldsymbol{\Lambda}$ is a vector of three multipliers, called the striction, which are associated with the inextensibility constraint (2.4.7). For a given state $\boldsymbol{z}=(\boldsymbol{r},\boldsymbol{q},\boldsymbol{\chi},\boldsymbol{\gamma})$, the striction $\boldsymbol{\Lambda}=\tilde{\boldsymbol{\Lambda}}(\boldsymbol{z})$ is required to satisfy the system of three elliptic ordinary differential equations

$$
\begin{aligned}
\boldsymbol{0} &= -\rho^{-1}(\boldsymbol{\chi}+\boldsymbol{\Lambda}_s)_s + I_j^{-1}\left(\tfrac{1}{2}\boldsymbol{B}_j\boldsymbol{q}\cdot\boldsymbol{\gamma}+\epsilon_{ij3}\boldsymbol{d}_i\cdot\boldsymbol{\Lambda}\right)\epsilon_{ij3}\boldsymbol{d}_i \\
&= -\rho^{-1}(\boldsymbol{\chi}+\boldsymbol{\Lambda}_s)_s - I_1^{-1}\left(\tfrac{1}{2}\boldsymbol{B}_1\boldsymbol{q}\cdot\boldsymbol{\gamma}-\boldsymbol{d}_2\cdot\boldsymbol{\Lambda}\right)\boldsymbol{d}_2 \\
&\quad + I_2^{-1}\left(\tfrac{1}{2}\boldsymbol{B}_2\boldsymbol{q}\cdot\boldsymbol{\gamma}+\boldsymbol{d}_1\cdot\boldsymbol{\Lambda}\right)\boldsymbol{d}_1 \;, \qquad (3.3.4)
\end{aligned}
$$

subject to an appropriate set of boundary conditions. For example, periodic boundary conditions arise for a closed loop. It can be shown that the condition (3.3.4) on the striction is simply an enforcement of the time derivative of the constraint (2.4.7).

It follows from equation (3.3.1) that the Hamiltonian dynamics are given by

$$
\begin{aligned}
&(3.3.5)\quad \boldsymbol{r}_t = \frac{\delta H}{\delta\boldsymbol{\chi}} = \rho^{-1}(\boldsymbol{\chi}+\tilde{\boldsymbol{\Lambda}}_s) \;, \\
&(3.3.6)\quad \boldsymbol{q}_t = \frac{\delta H}{\delta\boldsymbol{\gamma}} = I_j^{-1}\left(\tfrac{1}{2}\boldsymbol{B}_j\boldsymbol{q}\cdot\boldsymbol{\gamma}+\epsilon_{ij3}\boldsymbol{d}_i\cdot\tilde{\boldsymbol{\Lambda}}\right)\tfrac{1}{2}\boldsymbol{B}_j\boldsymbol{q} \;, \\
&(3.3.7)\quad \boldsymbol{\chi}_t = -\frac{\delta H}{\delta\boldsymbol{r}} = \boldsymbol{0} \;, \\
&\qquad \boldsymbol{\gamma}_t = -\frac{\delta H}{\delta\boldsymbol{q}} = I_j^{-1}\left(\tfrac{1}{2}\boldsymbol{B}_j\boldsymbol{q}\cdot\boldsymbol{\gamma}+\epsilon_{ij3}\boldsymbol{d}_i\cdot\tilde{\boldsymbol{\Lambda}}\right)\left(\tfrac{1}{2}\boldsymbol{B}_i\boldsymbol{\gamma}-\epsilon_{ij3}\boldsymbol{D}_i[\boldsymbol{q}]\,\tilde{\boldsymbol{\Lambda}}\right) \\
&\qquad\qquad + W_{u_j}\left(\frac{2\boldsymbol{B}_j\boldsymbol{q}_s}{|\boldsymbol{q}|^2} + \frac{2\boldsymbol{B}_j\boldsymbol{q}\cdot\boldsymbol{q}_s}{|\boldsymbol{q}|^2}\frac{2q}{|\boldsymbol{q}|^2}\right) \\
&(3.3.8)\qquad\qquad + \left(W_{u_j}\frac{2\boldsymbol{B}_j\boldsymbol{q}}{|\boldsymbol{q}|^2}\right)_s \;,
\end{aligned}
$$

where W is a function of $\mathsf{u} - \hat{\mathsf{u}}$, the matrices $\boldsymbol{B}_j$ and $\boldsymbol{D}_j$ are defined by equations (2.6.9) – (2.6.11) and (2.6.16), and there is an implied summation in the j index. In the special case of linear elasticity, the Hamiltonian dynamics can be simplified using equation (2.4.6).

The Hamiltonian dynamics for an elastica are also simplified by the fact that $\boldsymbol{r}$ is an ignorable coordinate, i.e., $\boldsymbol{r}$ does appear explicitly in the Hamiltonian (3.3.1). Consequently we see from equation (3.3.7) that the conjugate momentum $\boldsymbol{\chi}$ is constant. Therefore instead of analyzing fourteen equations, it suffices to fix a value for $\boldsymbol{\chi}$, and then consider the reduced Hamiltonian system consisting of the eight equations (3.3.6) and (3.3.8).

Finally, we remark that one could consider other materially constrained rod models, such as a rod which is extensible but not shearable. In that case the system of three equations (3.3.4) would be replaced by only two elliptic equations for the strictions, together with an additional constitutive law relating the stress n_3 to the strain v_3.

3.4. Hamiltonian form of invariants of motion. For each of the Hamiltonian formulations above, we now list the known conservation laws in terms of the Hamiltonian state variables, together with their associated symmetries. For details of the derivations, we refer to [8]. Of course, in order that these quantities are actually invariants, the boundary terms must be such that the appropriate flux terms vanish.

One of the elegant features of a Hamiltonian formulation is that according to Noether's Theorem (cf., e.g., [30]), for each invariant of motion there exists a continuous symmetry. Perhaps the best known example is the invariance of the Hamiltonian itself for autonomous systems, in which t can be replaced by $t+\epsilon$. The knowledge of the invariants of motion can be important for both analytical and computational purposes. In numerical simulations, the invariants can be used to check the accuracy of a numerical approximation to a solution. Moreover, in section 5.2 we describe how the invariants can be exploited in order to formulate a well-posed boundary value problem governing the equilibria of a loop.

We begin by discussing the invariants of motion for the Hamiltonian system given in section 3.2 which arise without any assumptions about the material properties of the rod. For example, it is apparent from equation (3.2.7) that the three components of the total linear momentum

$$P_k \equiv \int \rho \boldsymbol{r}_t \cdot \boldsymbol{e}_k \, ds \,, \qquad k = 1,2,3 \tag{3.4.1}$$

are conserved. The conservation of linear momentum is associated with the translational symmetry in space in which $\boldsymbol{r}$ is replaced by $\boldsymbol{r} + \epsilon \boldsymbol{e}_k$. We denote the total angular momentum about the origin by

$$\boldsymbol{\Pi} \equiv \int \{\boldsymbol{\pi} + \boldsymbol{r} \times \boldsymbol{p}\} \, ds \tag{3.4.2}$$

and let $\Pi_k \equiv \mathbf{\Pi} \cdot \boldsymbol{e}_k$. In terms of the Hamiltonian variables,

$$\Pi_k = \int \left\{ \tfrac{1}{2} \boldsymbol{B}_k^o \boldsymbol{q} \cdot \boldsymbol{\zeta} + (\boldsymbol{r} \times \boldsymbol{p}) \cdot \boldsymbol{e}_k \right\} ds. \tag{3.4.3}$$

which is associated with the symmetry of rotation about the inertial axis $\boldsymbol{e}_k$.

The total linear and angular momentum are both integrals over the length of the rod. In contrast, there are two sets of pointwise invariants which arise due to our Euler parameter formulation, which have no clear physical interpretation. First, at each point s there is the invariant $\boldsymbol{q}(s) \cdot \boldsymbol{q}(s)$ for the Euler parameters which was discussed in section 2.6. This is associated with the invariance of the Hamiltonian under the transformation in which $\boldsymbol{\gamma}$ is replaced by $\boldsymbol{\gamma} + \epsilon \boldsymbol{q}$. In addition, $\boldsymbol{q}(s) \cdot \boldsymbol{\gamma}(s)$ is an invariant at each point s. The symmetry associated with $\boldsymbol{q}(s) \cdot \boldsymbol{\gamma}(s)$ is given by the group of transformations in which $\boldsymbol{q}$ is replaced by $(1+\epsilon)\boldsymbol{q}$, and $\boldsymbol{\gamma}$ is simultaneously replaced by $(1+\epsilon)^{-1}\boldsymbol{\gamma}$. In fact, one of the primary reasons for scaling the directors as we did for this model of rod dynamics was to obtain this second family of invariants.

The remaining two invariants were already discussed in section 2.5, and are associated with assumptions on the material properties of the rod. Translational symmetry with respect to arc-length s implies invariance of the linear impulse I, which can be written in Hamiltonian variables as

$$I \equiv \int \{ \boldsymbol{p} \cdot \mathbf{r}_s + \boldsymbol{\zeta} \cdot \boldsymbol{q}_s \} \, ds. \tag{3.4.4}$$

Suppose instead that the rod is isotropic, that is, it is symmetric with respect to rotation about the tangent vector $\boldsymbol{d}_3$. Then we can conclude the invariance of the isotropic angular momentum A which takes a very simple form in terms of the Hamiltonian state variables, namely

$$A = \int \tfrac{1}{2} \boldsymbol{B}_3 \boldsymbol{q} \cdot \boldsymbol{\zeta} \, ds. \tag{3.4.5}$$

For each of the invariants listed above for the extensible, shearable rod there is a corresponding invariant for the Hamiltonian system in section 3.3 governing the elastica, in which the variables $\boldsymbol{p}$ and $\boldsymbol{\zeta}$ are replaced by $\boldsymbol{\chi}$ and $\boldsymbol{\gamma}$, respectively. In particular, it follows immediately from equation (3.3.7) that the three components of the total linear impetus

$$X_k \equiv \int \boldsymbol{\chi} \cdot \boldsymbol{e}_k \, ds, \qquad k = 1, 2, 3 \tag{3.4.6}$$

are invariants of motion. Moreover, assuming periodic boundary conditions, it follows that the components of linear momentum (3.4.1) are also conserved. In addition, for the elastica there is a family of pointwise invariants $\boldsymbol{r}_s(s) - \boldsymbol{d}_3(s)$ which describe the inextensibility condition. Associated with this family of invariants, the Hamiltonian formulation possesses a symmetry linked to the strictions $\boldsymbol{\Lambda}$, in which $\boldsymbol{\chi}$ is replaced by $\boldsymbol{\chi}+\boldsymbol{\Lambda}^*_s$, $\boldsymbol{\gamma}$ is replaced by $\boldsymbol{\gamma}+\boldsymbol{D}_3[\boldsymbol{q}]\,\boldsymbol{\Lambda}^*$, and $\boldsymbol{\Lambda}$ is replaced by $\boldsymbol{\Lambda}+\boldsymbol{\Lambda}^*$, where $\boldsymbol{\Lambda}^*$ is an arbitrary function of the arc-length s.

4. Hamiltonian formulations of statics.

4.1. Introduction. In this chapter we present various Hamiltonian formulations describing rod statics, for both unconstrained and constrained theories. Each of the Hamiltonian systems in this chapter can be expressed as

$$\boldsymbol{z}_s = \boldsymbol{J}\,\nabla H(\boldsymbol{z}) \;, \tag{4.1.1}$$

where the matrix $\boldsymbol{J}$ is again given by (3.1.2). The structure of equation (4.1.1) is very similar to that of equation (3.1.1) for time dynamics. However in equation (4.1.1), $\boldsymbol{z}$ is a function of s only, H is the energy density at a point s (and not an integral), and the variational derivative δ appearing in equation (3.1.1) is replaced by the gradient ∇ with respect to $\boldsymbol{z}$. Thus the Hamiltonian system given by (4.1.1) is a system of ordinary differential equations which evolve in s. We remark that in statics, in contrast with the situation in dynamics, the analysis of constrained rods is easier than the analysis of unconstrained rods.

This chapter parallels the development of chapter 3. Once again, for simplicity we assume there are no external loads. In sections 4.2 and 4.3 we present Hamiltonian formulations describing the statics of an extensible, shearable rod and an elastica, respectively. In each case we begin with the formulation for a general strain energy density, then specialize to the case of linear elasticity. The two Hamiltonian formulations have very similar structures, and have the same integrals, which are presented in section 4.4.

4.2. Hamiltonian formulation of the statics of an extensible, shearable rod. In the general case of an extensible, shearable rod, where the strain energy is given by $W(\mathsf{u}-\hat{\mathsf{u}},\mathsf{v}-\hat{\mathsf{v}})$, the Hamiltonian is

$$H(\boldsymbol{r},\boldsymbol{q},\boldsymbol{n},\boldsymbol{\mu}) = W^*(\mathsf{m},\mathsf{n}) + \hat{u}_j m_j + \boldsymbol{n}\cdot\boldsymbol{d}_3 \;. \tag{4.2.1}$$

where W^* denotes the Legendre transform of the strain energy density W, $\mathsf{m}=(m_1,m_2,m_3)$ and $\mathsf{n}=(n_1,n_2,n_3)$. (See [1], for example, for a definition of the Legendre transform.) Notice that now the Hamiltonian (4.2.1) is a scalar-valued function, while in contrast the Hamiltonians (3.2.1) and (3.3.1) are integrals over the rod, yielding the partial differential equations describing the dynamics of rods. In this Hamiltonian formulation, the force $\boldsymbol{n}$ is the variable conjugate to $\boldsymbol{r}$, while the variable $\boldsymbol{\mu}$ conjugate to the Euler parameters $\boldsymbol{q}$ is defined by

$$\boldsymbol{\mu} \equiv W_{u_j}(\mathsf{u}-\hat{\mathsf{u}})\,\frac{2}{|\mathbf{q}|^2}\boldsymbol{B}_j\boldsymbol{q} + \nu\boldsymbol{q} \;, \tag{4.2.2}$$

where u is given in terms of $\boldsymbol{q}$ by equation (2.6.22) and ν has the same meaning as in section 3.2. Accordingly, each component of moment $m_j = W_{u_j}$ is given in terms of the Hamiltonian variables by

$$m_j = \tfrac{1}{2}\boldsymbol{B}_j\boldsymbol{q}\cdot\boldsymbol{\mu}\ . \tag{4.2.3}$$

The associated Hamiltonian system is

$$\boldsymbol{r}_s = \frac{\partial H}{\partial \boldsymbol{n}} = W^*_{n_j}\boldsymbol{d}_j + \boldsymbol{d}_3\ , \tag{4.2.4}$$
$$\boldsymbol{q}_s = \frac{\partial H}{\partial \boldsymbol{\mu}} = \left(W^*_{m_j} + \hat{u}_j\right)\tfrac{1}{2}\boldsymbol{B}_j\boldsymbol{q}\ , \tag{4.2.5}$$
$$\boldsymbol{n}_s = -\frac{\partial H}{\partial \boldsymbol{r}} = \boldsymbol{0}\ , \tag{4.2.6}$$
$$\boldsymbol{\mu}_s = -\frac{\partial H}{\partial \boldsymbol{q}} = \left(W^*_{m_j} + \hat{u}_j\right)\tfrac{1}{2}\boldsymbol{B}_j\boldsymbol{\mu} - W^*_{n_j}\boldsymbol{D}_j[\boldsymbol{q}]\,\boldsymbol{n} - \boldsymbol{D}_3[\boldsymbol{q}]\,\boldsymbol{n}\ , \tag{4.2.7}$$

where W^* is a function of m and n, the matrices $\boldsymbol{B}_j$ and $\boldsymbol{D}_j$ are defined by equations (2.6.9) – (2.6.11) and (2.6.16), and there is an implied summation in the j index.

In the special case of linear elasticity where the strain energy density W is given by (2.4.4), the Legendre transform is

$$W^*(\mathsf{m},\mathsf{n}) = \tfrac{1}{2}K_j^{-1}m_j^2 + \tfrac{1}{2}A_j^{-1}n_j^2\ , \tag{4.2.8}$$

so the Hamiltonian system is

$$\boldsymbol{r}_s = \frac{\partial H}{\partial \boldsymbol{n}} = A_j^{-1}\left(\boldsymbol{n}\cdot\boldsymbol{d}_j\right)\boldsymbol{d}_j + \boldsymbol{d}_3\ , \tag{4.2.9}$$
$$\boldsymbol{q}_s = \frac{\partial H}{\partial \boldsymbol{\mu}} = \left[K_j^{-1}\left(\tfrac{1}{2}\boldsymbol{B}_j\boldsymbol{q}\cdot\boldsymbol{\mu}\right) + \hat{u}_j\right]\tfrac{1}{2}\boldsymbol{B}_j\boldsymbol{q}\ , \tag{4.2.10}$$
$$\boldsymbol{n}_s = -\frac{\partial H}{\partial \boldsymbol{r}} = \boldsymbol{0}\ , \tag{4.2.11}$$
$$\begin{aligned}\boldsymbol{\mu}_s = -\frac{\partial H}{\partial \boldsymbol{q}} &= \left[K_j^{-1}\left(\tfrac{1}{2}\boldsymbol{B}_j\boldsymbol{q}\cdot\boldsymbol{\mu}\right) + \hat{u}_j\right]\tfrac{1}{2}\boldsymbol{B}_j\boldsymbol{\mu} \\ &\quad - A_j^{-1}\left(\boldsymbol{n}\cdot\boldsymbol{d}_j\right)\boldsymbol{D}_j[\boldsymbol{q}]\,\boldsymbol{n} - \boldsymbol{D}_3[\boldsymbol{q}]\boldsymbol{n}\ .\end{aligned} \tag{4.2.12}$$

4.3. Hamiltonian formulation of the statics of an elastica. For an inextensible, unshearable rod, where the strain energy is given by $W(\mathsf{u} - \hat{\mathsf{u}})$, the Hamiltonian is

$$H(\boldsymbol{r},\boldsymbol{q},\boldsymbol{n},\boldsymbol{\mu}) = W^*(\mathsf{m}) + \hat{u}_j m_j + \boldsymbol{n}\cdot\boldsymbol{d}_3\ . \tag{4.3.1}$$

The associated Hamiltonian system is

$$\boldsymbol{r}_s = \frac{\partial H}{\partial \boldsymbol{n}} = \boldsymbol{d}_3\ , \tag{4.3.2}$$

$$
\begin{aligned}
&(4.3.3) \qquad & \boldsymbol{q}_s = \ & \frac{\partial H}{\partial \boldsymbol{\mu}} & = \ & \left(W^*_{m_j} + \hat{u}_j\right) \tfrac{1}{2}\boldsymbol{B}_j \boldsymbol{q} \ , \\
&(4.3.4) \qquad & \boldsymbol{n}_s = - & \frac{\partial H}{\partial \boldsymbol{r}} & = \ & \boldsymbol{0} \ , \\
&(4.3.5) \qquad & \boldsymbol{\mu}_s = - & \frac{\partial H}{\partial \boldsymbol{q}} & = \ & \left(W^*_{m_j} + \hat{u}_j\right) \tfrac{1}{2}\boldsymbol{B}_j \boldsymbol{\mu} - \boldsymbol{D}_3[\boldsymbol{q}]\boldsymbol{n} \ ,
\end{aligned}
$$

where the matrices $\boldsymbol{B}_j$ and $\boldsymbol{D}_j$ are defined by equations (2.6.9) – (2.6.11) and (2.6.16), and there is an implied summation in the j index. In the special case where the strain energy density W is given by (2.4.9), the Legendre transform is

$$
(4.3.6) \qquad W^*(\mathsf{m}) = \tfrac{1}{2} K_j^{-1} m_j^2 \ ,
$$

so the Hamiltonian system is

$$
\begin{aligned}
&(4.3.7) \qquad & \boldsymbol{r}_s = \ & \frac{\partial H}{\partial \boldsymbol{n}} & = \ & \boldsymbol{d}_3 \ , \\
&(4.3.8) \qquad & \boldsymbol{q}_s = \ & \frac{\partial H}{\partial \boldsymbol{\mu}} & = \ & \left(K_j^{-1} m_j + \hat{u}_j\right) \tfrac{1}{2}\boldsymbol{B}_j \boldsymbol{q} \ , \\
&(4.3.9) \qquad & \boldsymbol{n}_s = - & \frac{\partial H}{\partial \boldsymbol{r}} & = \ & \boldsymbol{0} \ , \\
&(4.3.10) \qquad & \boldsymbol{\mu}_s = - & \frac{\partial H}{\partial \boldsymbol{q}} & = \ & \left(K_j^{-1} m_j + \hat{u}_j\right) \tfrac{1}{2}\boldsymbol{B}_j \boldsymbol{\mu} - \boldsymbol{D}_3[\boldsymbol{q}]\boldsymbol{n} \ .
\end{aligned}
$$

Notice that the strain energy term (4.2.8) for the extensible, shearable rod differs from the corresponding term (4.3.6) for the elastica only in its second term, which measures the energy due to stretching and shearing. In particular, in the limit as the coefficients A_j approach infinity (i.e., as the rod becomes inextensible and unshearable), the unconstrained Hamiltonian approaches the constrained Hamiltonian.

As in the case of the dynamics discussed in section 3.4, the two Hamiltonian formulations of statics are simplified by the fact that $\boldsymbol{r}$ is an ignorable coordinate. As a consequence, instead of analyzing fourteen equations, one can fix the value of the force $\boldsymbol{n}$, and then consider the reduced Hamiltonian system consisting of only eight equations given by (4.2.5) and (4.2.7) for an extensible, shearable rod or the analogous system (4.3.3) and (4.3.5) for an elastica.

4.4. Hamiltonian form of integrals for statics. We now describe the integrals arising in the Hamiltonian system of ordinary differential equations describing the statics of rods, together with their associated symmetries. The discussion parallels that given in section 3.4 for the Hamiltonian system of partial differential equations modelling dynamics.

It turns out that the integrals arising for the extensible, shearable rod and for the elastica are identical, so we will only explicitly refer to the extensible, shearable case. Moreover, as was discussed in section 2.5, four of the integrals of the statics of rod are related to the invariants of motion through the conservation laws (2.5.5), (2.5.7), (2.5.11), and (2.5.17). (As was pointed out in section 2.5, the integral arising from the remaining conservation law (2.5.9) is trivial. The reason for this is that the symmetry associated with (2.5.9) is translation in time, which implies the conservation of total energy in the case of dynamics, but has no significance in the case of statics.)

The three components of force $\boldsymbol{n}$ are also constant, due to the translational symmetry of the Hamiltonian system in space. This fact is directly related to the invariance of the three components of total linear momentum (3.4.1), through the conservation law (2.5.5). Similarly the three components of $\boldsymbol{m} + \boldsymbol{r} \times \boldsymbol{n}$ are integrals as a consequence of rotational symmetry about the three inertial axes, which is also associated with the invariance of total angular momentum via equation (2.3.6).

In addition to the integrals listed above which have physical interpretations, there are two integrals which arise from the representation of $SO(3)$ by Euler parameters. The quantity $\boldsymbol{q} \cdot \boldsymbol{q}$ is an integral by the construction of the Hamiltonian formulation, just as in the case of dynamics, and is associated with the invariant of the Hamiltonian under to the transformation in which $\boldsymbol{\mu}$ is replaced by $\boldsymbol{\mu} + \epsilon \boldsymbol{q}$. The quantity $\boldsymbol{\mu} \cdot \boldsymbol{q} + 2\boldsymbol{r} \cdot \boldsymbol{n}$ is also an integral. By contrast, the analogous quantity $\boldsymbol{\zeta} \cdot \boldsymbol{q} + 2\boldsymbol{r} \cdot \boldsymbol{n}$ is *not* an invariant in the case of dynamics; rather we have shown that $\boldsymbol{\zeta} \cdot \boldsymbol{q}$ is invariant. The difference arises from the scaling factor $1/|\boldsymbol{q}|^2$ applied to the Euler parameter representation of the directors. In dynamics, the additional factor was included in the model in order to obtain an additional invariant. But in statics it is not needed, so to conform with common practice in the kinematics literature the factor is omitted. The constancy of $\boldsymbol{\mu} \cdot \boldsymbol{q} + 2\boldsymbol{r} \cdot \boldsymbol{n}$ is associated with the invariance of the Hamiltonian (4.2.1) under the transformation in which $\boldsymbol{q}$ is replaced by $(1+\epsilon)\boldsymbol{q}$, $\boldsymbol{\mu}$ is replaced by $(1+\epsilon)^{-1}\boldsymbol{\mu}$, $\boldsymbol{r}$ is replaced by $(1+\epsilon)^2\boldsymbol{r}$ and $\boldsymbol{n}$ is replaced by $(1+\epsilon)^{-2}\boldsymbol{n}$.

The above integrals arise for all constitutive laws. As before there are two additional, constitutive dependent integrals that arise in each of the cases of a uniform rod, and an isotropic rod. If we assume the rod is translationally symmetric in the arc-length s, then the Hamiltonian H (4.2.1) is an integral. The constancy of H is associated with the invariance of the linear impulse I (2.5.12) through the conservation law (2.5.11). Finally, for isotropic rods $\boldsymbol{m} \cdot \boldsymbol{d}_3$ is an integral in the case of statics, which is linked to the invariance of the isotropic angular momentum (2.5.18) in the case of dynamics through the conservation law (2.5.17).

There is a well developed theory of integrability in Hamiltonian systems of ordinary differential equations. The classic result is that a Hamiltonian system with N degrees of freedom (i.e. $2N$ equations) is completely integrable if there are N linearly independent integrals in involution. Two integrals I_1 and I_2 are said to commute, or be in involution, if the Poisson bracket $\{I_1, I_2\} \equiv \nabla I_1 \cdot \boldsymbol{J} \nabla I_2$ vanishes identically. The N integrals are in involution if all their Poisson brackets vanish identically. We have already shown that there are always eight linearly independent (i.e. different) integrals for our seven degree of freedom Hamiltonian system describing rod statics, and that the symmetries of a uniform, and of an isotropic rod add a ninth and tenth linearly independent integral. A lengthy, but straightforward, calculation (which, because our integrals are all simple polynomials, can be efficiently carried out by a symbolic manipulation package such as Maple or Mathematica) reveals that of the eight integrals only five commute, but that of the ten integrals, seven are in involution. Thus the uniform, isotropic rod is the only (known) case of complete integrability. One of the main consequences of complete integrability is the conclusion that there is a choice of coordinates (unfortunately not defined constructively) in which the initial value problem can in principle be completely solved by quadrature. In the case of a twist–free, unshearable, inextensible rod (and using Euler angles rather than Euler parameters to parameterize $SO(3)$) the appropriate calculations are carried out in [22] (§19). The twisted integrable case and many more calculations are considered in [17] (see also [39] and [38]). The key step is to use cylindrical coordinates to describe the axes of the rod, with the centerline of the cylinder aligned with the direction of the shear force.

The explicit coordinates for integration of the rod equilibrium equations were independently rediscovered by Langer and Singer [23] from a very different, rather geometrical point of view, and subsequently detailed calculations were carried out and applied within the context of DNA modelling by Shi and Hearst [32]. All of these cited works considered only the unshearable, inextensible elastica model. However the Hamiltonian integrability analysis presented here is identical for the elastica and the shearable, extensible rod, so solution by quadrature should be possible in both cases. And indeed in a contemporaneous preprint [31] Shi, Borovik and Hearst have carried out the quadrature for shearable, extensible rods.

It should be understood that a solution by quadrature involves a number of free constants. In an initial value problem, where all the variables are assigned values at $s = 0$, the values of all these constants are typically determined, so that the quadrature is indeed a closed form solution. Initial value problems naturally arise in classic applications of finite dimensional Hamiltonian systems where the independent variable is time. However in the DNA context the independent variable is arc-length, and a two-point boundary value problem arises naturally. In other words, some variables are assigned values at $s = 0$, and some are assigned values at $s = 1$. For such problems a solution by quadrature is not truly explicit, for the values of at least some of the integration constants cannot typically be determined analytically. Accordingly, we are of the opinion that a quadrature solution is of rather limited utility in the solution of the boundary value problems arising in the modelling of DNA. This viewpoint is further expounded in Chapter 5.

In fact the accurate numerical solution of an initial value problem is so straightforward with contemporary machines and software packages, that the use of the solution by quadrature is typically not even an efficient way to numerically generate solutions. In particular, details of various packages developed by K.A. Rogers and R.C. Paffenroth with numerics linked to interactive graphics for examining solutions of the initial value problem for rod equilibria can be found at the World Wide Web URL http://www.glue.umd.edu/~karogers/slinky.html .

5. Equilibria of a closed, twisted elastic loop.

5.1. Introduction. In this section we present a brief description of some recent analytical and computational results regarding the analysis of the set of equilibria of a closed, twisted loop. This work is fully described in the sequence of articles [25], [26] and [27] (see also the WWW URL http://jacobi.umd.edu/). The example of a closed elastic rod has now received considerable attention as a very simple, but prototypical model for supercoiling of DNA (see, for example [2], [4], [19], [24], [34], [31], [32], [38], [40], [41], references therein, other articles in this volume, and the extensive survey by Schlick [33]).

The novelty in our treatment is that we exploit the Hamiltonian formulation of the two-point boundary value problem for ordinary differential equations governing equilibria to construct an efficient numerical approach that explicitly takes account of all the symmetries of the problem. In particular, we do not use the Lk = Tw + Wr formula, which would restrict attention to isotropic rods, nor do we use the semi-explicit solution to the initial value problem which, in addition to being computationally inefficient, would restrict attention to the integrable case of a uniform, isotropic rod. As a consequence we can compute equilibria for rather general classes of rods.

Indeed for our approach, which uses parameter continuation, the integrable case is in a sense the hardest to compute. The symmetries of the integrable problem give rise, in both the unshearable, inextensible and shearable, extensible cases, to a closed form 'trivial' solution in which the centerline of the rod is a circle and the cross-sections are uniformly twisted. This closed form solution serves as a convenient starting point for our numerical continuation techniques. The potential difficulty is that the same symmetries which give rise to this special solution also imply that all solutions are nonisolated for a given load parameter (i.e. for prescribed twist, shear force or link). This non-isolation necessitates some care in the numerical continuation approach.

In fact the same symmetries that give rise to the difficulties associated with non-isolation also provide the means to resolve the problem. It was noted in section 3.4 that in a Hamiltonian formulation, or any variational formulation, symmetries generate integrals of the ordinary differential equations. These integrals act to convect information from $s = 0$ to

$s = 1$ with the consequence that some boundary conditions at $s = 1$ are actually implied by boundary conditions at $s = 0$. The upshot is that some boundary conditions are actually implied and can be replaced by additional boundary conditions that factor out the non-isolation in such a way that a numerically well-posed boundary value problem remains.

The benefits of treating the integrable case in this careful fashion are two-fold. First, the complete solution set is obtained for both the shearable, extensible and unshearable, inextensible cases, for arbitrary ratios K_3/K_1 of twisting stiffness to bending stiffness, and for arbitrary values of the unstressed twist $\hat{u}_3$. Second, any solution for the integrable case can be used as a starting point for parameter continuation in the coefficients, with the consequence that all the non-integrable cases can also be computed. In particular, when the model is modified to include a pairwise potential of the form (2.3.7) that prevents self-intersection of the rod, equilibria of a prescribed torus knot type and prescribed linking number can be computed for non-uniform rods with arbitrary unstressed configuration and bend, twist, shear and extension coefficients. We defer to the sequence of papers [25], [26], and [27] and to [13] for a full account of these results, and will here restrict attention to a description of the solution set for the integrable case.

Both the analytic form of the circular solution and the computation of nonplanar equilibria for a shearable, extensible rod we believe to be original. The analytic form of the circular solution in the unshearable, inextensible case is by now well-known, but we believe our computation of the higher modes of the solution set, and of the general pattern of connectivity to be original. The higher modes are of some interest because experiments with highly flexible wires indicate that when effects of self-contact are included, some of the $(M + N)$-foil solutions are stable at least for $(M + N) \leq 14$. We also remark that the rod example described here formed the primary motivation for the development of an interactive graphics package that allows the display of bifurcation sets and associated solutions for two-point boundary value problems [14] (see also the WWW URL http://jacobi.umd.edu/pcr.html).

5.2. The boundary value problem. Consider a uniform, isotropic, linearly elastic rod, so that $\hat{u}_1 = \hat{u}_2 = 0$, $K_2 = K_1$ and for a shearable rod $A_2 = A_1$. In the statics of rods the equilibrium equations can be nondimensionalized with respect to both a length scale and a force scale. Thus we may assume with no loss of generality that the undeformed arc-length is one, $0 \leq s \leq 1$, and that $K_1 = 1$. Note that we can allow an initial natural twist $\hat{u}_3 \neq 0$, but that with our nondimensionalization $\hat{u}_3$ may assume an effective continuum of values that is scaled by the number of base pairs in the segment of DNA. In the case of an unshearable, inextensible rod (i.e. an elastica) there is only one free additional parameter, namely the nondimensionalized value of K_3 (or equivalently the ratio K_3/K_1). In point of fact using the symmetry of isotropy it is straightforward to verify that as $\hat{u}_3$ and K_3 are varied the axis (or centerline) of any equilibrium is unchanged, and the directors merely rotate about the tangent vector at a different (and explicitly determined) constant rate. In this sense a computation of the equilibria for any values of $\hat{u}_3$ and K_3, contains practically all the information for a solution with general values.

The equilibrium conditions are a set of fourteen nonlinear ordinary differential equations, and to be able to straightforwardly apply numerical continuation we must find a set of fourteen boundary conditions and one free parameter, such that at (most) fixed parameter values the solutions of the boundary value problem are locally isolated. The boundary conditions should imply that the centerline closes on itself smoothly, and, in order to obtain local isolation, that the symmetries of translation in space, translation in arc-length, rotations in space, and rotations of the rod about its centerline are all eliminated. As detailed in [25] and [27] for the unshearable and shearable cases respectively, the Hamiltonian form of the equilibrium conditions and the associated integrals can be used to demonstrate that an appropriate set of boundary conditions is:

$$\boldsymbol{r}(0) = (0,0,0)^T \ , \tag{5.2.1}$$

$$\boldsymbol{r}_s(0)\cdot\boldsymbol{e}_1 = 0 \ , \tag{5.2.2}$$

$$|\boldsymbol{q}(0)|^2 = 1 \ , \tag{5.2.3}$$

$$q_1(0) = 0 \ , \tag{5.2.4}$$

$$q_3(0) = 0 \ , \tag{5.2.5}$$

$$\boldsymbol{\mu}(0)\cdot\boldsymbol{q}(0) = 0 \ , \tag{5.2.6}$$

$$\boldsymbol{r}(1) = (0,0,0)^T \ , \tag{5.2.7}$$

$$\boldsymbol{n}(1) = (\lambda,0,0)^T \ . \tag{5.2.8}$$

Here

$$\boldsymbol{r}_s(0) = \boldsymbol{d}_3(0) + \frac{\boldsymbol{n}(0)\cdot\boldsymbol{d}_j(0)}{A_j}\boldsymbol{d}_j(0) \ , \tag{5.2.9}$$

the free parameter is the magnitude of the shear force λ and summation in j is implied. At first sight it might seem more natural to have the free parameter be ΔLk (or equivalently the angle between $\boldsymbol{d}_1(0)$ and $\boldsymbol{d}_1(1)$) or the magnitude of the twisting component of the moment, but it turns out that they are all essentially equivalent for the purposes of constructing one parameter families of solutions. As written (5.2.1) – (5.2.8) are for the shearable case, but to obtain the appropriate unshearable boundary conditions one merely sends the coefficients A_j appearing in (5.2.9) to infinity.

One can show that the boundary conditions (5.2.1) – (5.2.8) are satisfied by the following 'trivial' solutions of the equilibrium equations. The centerline in each solution is a multiply covered circle (covered an integer

N times) lying in the (y, z) plane with $y \leq 0$ and the tangent at $s = 0$ lying along the z-axis. The $\boldsymbol{d}_3$ director makes a constant angle α with the (y, z)-plane, and the other directors uniformly rotate about it with a constant spin rate. The shear angle α must satisfy the relation

$$\sin\alpha = \frac{-2\,(\lambda/A_1)}{1+\sqrt{1+4\,(1-A_1/A_3)\,(\lambda/A_1)^2}}\,. \tag{5.2.10}$$

Then the centerline is given by

$$\boldsymbol{r}(s) = R\,(0,\ \cos 2\pi N s - 1,\ \sin 2\pi N s)^T\ , \tag{5.2.11}$$

where

$$R = \frac{1}{2\pi N\cos\alpha}\left(1+\frac{\lambda\sin\alpha}{A_3}\right)\,. \tag{5.2.12}$$

The directors are

$$\boldsymbol{d}_1(s) = \begin{pmatrix} \cos\alpha\,\cos\omega s \\ \sin\omega s\,\cos 2\pi N s + \sin\alpha\,\cos\omega s\sin 2\pi N s \\ \sin\omega s\,\sin 2\pi N s - \sin\alpha\,\cos\omega s\,\cos 2\pi N s \end{pmatrix}\ , \tag{5.2.13}$$

$$\boldsymbol{d}_2(s) = \begin{pmatrix} -\cos\alpha\,\cos\omega s \\ \cos\omega s\,\cos 2\pi N s - \sin\alpha\,\sin\omega s\,\sin 2\pi N s \\ \cos\omega s\,\sin 2\pi N s + \sin\alpha\,\sin\omega s\,\cos 2\pi N s \end{pmatrix}\ , \tag{5.2.14}$$

$$\boldsymbol{d}_3(s) = \begin{pmatrix} \sin\alpha \\ -\cos\alpha\,\sin 2\pi N s \\ \cos\alpha\,\cos 2\pi N s \end{pmatrix}\ , \tag{5.2.15}$$

in which the twist rate ω is related to the force λ through

$$\omega = \frac{\lambda R}{N K_3\cos\alpha} + \left(\frac{K_1}{K_3} - 1\right) 2\pi N\sin\alpha\ , \tag{5.2.16}$$

and the associated Euler parameters are

$$q_1(s) = \cos\frac{\alpha}{2}\,\sin\pi N s\,\cos\frac{\omega s}{2} + \sin\frac{\alpha}{2}\,\cos\pi N s\,\sin\frac{\omega s}{2}\ , \tag{5.2.17}$$

$$q_2(s) = -\cos\frac{\alpha}{2}\,\sin\pi N s\,\sin\frac{\omega s}{2} + \sin\frac{\alpha}{2}\,\cos\pi N s\,\cos\frac{\omega s}{2}\ , \tag{5.2.18}$$

$$q_3(s) = \cos\frac{\alpha}{2}\,\cos\pi N s\,\sin\frac{\omega s}{2} + \sin\frac{\alpha}{2}\,\sin\pi N s\,\cos\frac{\omega s}{2}\ , \tag{5.2.19}$$

$$q_4(s) = \cos\frac{\alpha}{2}\,\cos\pi N s\,\cos\frac{\omega s}{2} - \sin\frac{\alpha}{2}\,\sin\pi N s\,\sin\frac{\omega s}{2}\ . \tag{5.2.20}$$

Finally, the impetuses μ_j associated with the Euler parameters are given by

$$\mu_1(s) = \left(4\pi N K_1\cos\frac{\alpha}{2} + \frac{2\lambda R}{N\cos\alpha}\sin\frac{\alpha}{2}\right)\cos\pi N s\,\cos\frac{\omega s}{2}$$

$$-\left(4\pi N K_1 \sin\frac{\alpha}{2} + \frac{2\lambda R}{N\cos\alpha}\cos\frac{\alpha}{2}\right)\sin\pi N s\,\sin\frac{\omega s}{2}\,, \tag{5.2.21}$$

$$\begin{aligned}\mu_2(s) \;=\; & -\left(4\pi N K_1 \cos\frac{\alpha}{2} + \frac{2\lambda R}{N\cos\alpha}\sin\frac{\alpha}{2}\right)\cos\pi N s\,\sin\frac{\omega s}{2}\\ & -\left(4\pi N K_1 \sin\frac{\alpha}{2} + \frac{2\lambda R}{N\cos\alpha}\cos\frac{\alpha}{2}\right)\sin\pi N s\,\cos\frac{\omega s}{2}\,,\end{aligned} \tag{5.2.22}$$

$$\begin{aligned}\mu_3(s) \;=\; & -\left(4\pi N K_1 \cos\frac{\alpha}{2} + \frac{2\lambda R}{N\cos\alpha}\sin\frac{\alpha}{2}\right)\sin\pi N s\,\sin\frac{\omega s}{2}\\ & +\left(4\pi N K_1 \sin\frac{\alpha}{2} + \frac{2\lambda R}{N\cos\alpha}\cos\frac{\alpha}{2}\right)\cos\pi N s\,\cos\frac{\omega s}{2}\,,\end{aligned} \tag{5.2.23}$$

$$\begin{aligned}\mu_4(s) \;=\; & -\left(4\pi N K_1 \cos\frac{\alpha}{2} + \frac{2\lambda R}{N\cos\alpha}\sin\frac{\alpha}{2}\right)\sin\pi N s\,\cos\frac{\omega s}{2}\\ & -\left(4\pi N K_1 \sin\frac{\alpha}{2} + \frac{2\lambda R}{N\cos\alpha}\cos\frac{\alpha}{2}\right)\cos\pi N s\,\sin\frac{\omega s}{2}\,.\end{aligned} \tag{5.2.24}$$

In the inextensible, unshearable limit, where the coefficients $\{A_j\}$ go to infinity, the shear angle α given by (5.2.10) goes to zero. In this limit, the expressions (5.2.11) – (5.2.24) above yield the corresponding values for the classic solution of the inextensible, unshearable rod.

The only other planar equilibria of the boundary value problem (5.2.1) – (5.2.8) are found by reflecting the above solution in the (x, z)-plane. The magnitude of the force is unaltered in the reflection, but being a mirror image the sign of the twist is reversed. Accordingly we refer to the original family as $+$ solutions, and to the reflected family as $-$ solutions. (Cf. Figure 5.2.)

5.3. Nonplanar equilibria. Both analytical and computational methods can be applied to show that a number of non-planar equilibria bifurcate (or branch) from the above described solutions at certain critical load parameters. In fact on each trivial branch there is a countable infinity of simple bifurcation points which may therefore be indexed as $(M, N, \pm)$ where M indicates the first, second, third, etc. bifurcation point on the N covered solution with either positive or negative twist. The main point of interest is to follow the branches of non-planar equilibria emanating from the known circular solutions. That procedure must be done numerically, even given the semi-explicit solution of the initial value problem that was discussed at the end of the previous chapter. Indeed Starotsin [38] combined the quadrature solution with a root solving algorithm for the undetermined constants of integration to trace out some (apparently partial) branches in the case of an unshearable rod. Shi & Hearst [32] also use the quadrature solution for an unshearable rod to calculate some isolated solutions, and in [31] an analogous solution by quadrature was found for the shearable extensible rod. However, in this last work no solutions to the two-point boundary value problem are computed due to the complexity of the quadrature formulæ. As remarked previously we regard the *ab initio* numerical generation of solutions to the initial value problem as straightforward computationally, and given the particular solution described in the previous section we also regard the numerical solution of the two-point boundary value problem as routine once the appropriate boundary conditions have been identified. Morever although we will not describe the detailed results here, a direct numerical approach extends to treat non-integrable cases (such as arise for example in the modelling of naturally curved DNA) in both the shearable and unshearable contexts.

We chose to use the package AUTO [12], which uses parameter continuation combined with a discretization based on the collocation method. The known trivial circular solution for the isotropic, uniform rod is used as as a starting point, then a continuation method is applied to numerically trace the bifurcating branches of non-planar equilibria. The result that was rather surprising to us was that the branch emanating from the Mth bifurcation on the N-covered ring with positive twist links to the Nth bifurcation point on the M-covered ring with negative twist, written symbolically as $(M, N, +) \leftrightarrow (N, M, -)$. Moreover, the only instance where the rod has any self-intersection is at a single point on each branch, where an $(M+N)$-foil arises, i.e. a symmetrical configuration with $M+N$ leaves. In fact the centerline of the nonplanar solutions is wound on a torus (or doughnut) in three-space with the cross-section of the torus deforming as the parameter varies. The integers (M, N) determine the torus knot type of the centerline, which is also inherited from the eigenfunction of the eigensolution to the linearized problem at the bifurcation point. The $(M+N)$-foil arises when the hole in the doughnut pinches off at one critical parameter value. The knot type switches at this point, and it is also close to this point that the numerics can be switched to a code that includes a model to preclude self-intersection. For the unshearable rod, this behavior was known in the case $(M + N) = 2$ where the 2-foil is the figure eight, but for $(M + N) > 3$ we believe the conclusion to be original, with the case $(M+N) = 3$ being partially understood previously [34]. The fact that the same behavior also arises for shearable rods was apparently unrealised, but is perhaps unsurprising.

In understanding the results of our bifurcation analysis we have found it extremely valuable to display the results of our computations using an interactive graphics package called PCR [14]. The full benefits of this graphics utility can only be appreciated with the interactive capabilities of a graphics workstation, but we have included some illustrations that depict some of the output. Figures 5.1–5.7 all illustrate certain features of the DNA supercoiling problem. These figures were obtained for the inextensible, unshearable case, but the features are unchanged to the eye for a surprisingly large range of extensible, shearable rods. Figures 5.1, 5.3, 5.4, 5.5, 5.6 and 5.7 each comprise four viewpoints of a single equilibrium of a rod. The four views comprise two elevations, a plan view and a skew-view (the axes reveal the relative orientations of each viewpoint). Each Figure illustrates an equilibrium for a different amount of imposed twist. Figure 5.2 shows a sequence of different configurations on the $(1, 1)$ branch from a single skew perspective. Equilibria of the twisted ring problem arise in one-dimensional families as a load parameter, such as ΔLk, is varied. Figures 5.8 and 5.9 further illustrate the output of the package PCR with displays of certain associated bifurcation diagrams.

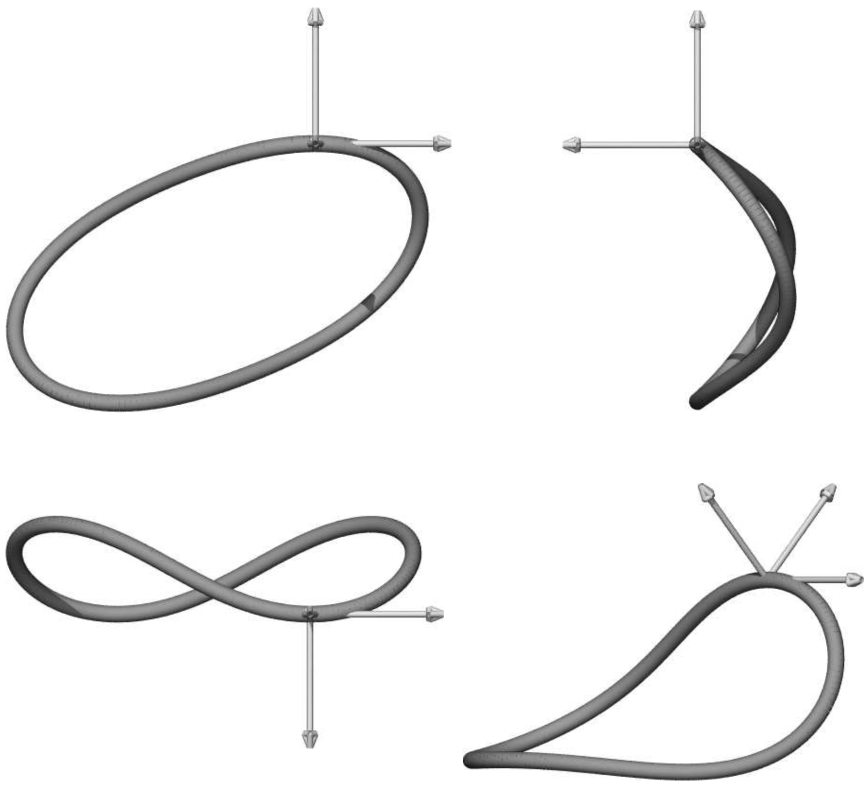

FIG. 5.1 *Four views of a typical configuration on the solution branch emanating from the* $(1, 1, +)$ *bifurcation point. It has left-right symmetry in both side elevations, and period two symmetry in the plan view. Domokos [13] provides a full account of the symmetries of ring equilibria.*

FIG. 5.2 *Different configurations all lying on the branch that links the* $(1,1,-)$ *and* $(1,1,+)$ *bifurcation points. The circle in the upper left is a negative twist solution, and the upper right solution is analogous to Figure 5.1. In the middle left there is a self-intersecting planar figure-eight solution, with another solution analogous to Figure 5.1 in the middle right, and finally the planar positive twist solution. The twist is monotone increasing from a negative to positive value through this sequence. In these calculations effects of self-intersection are ignored.*

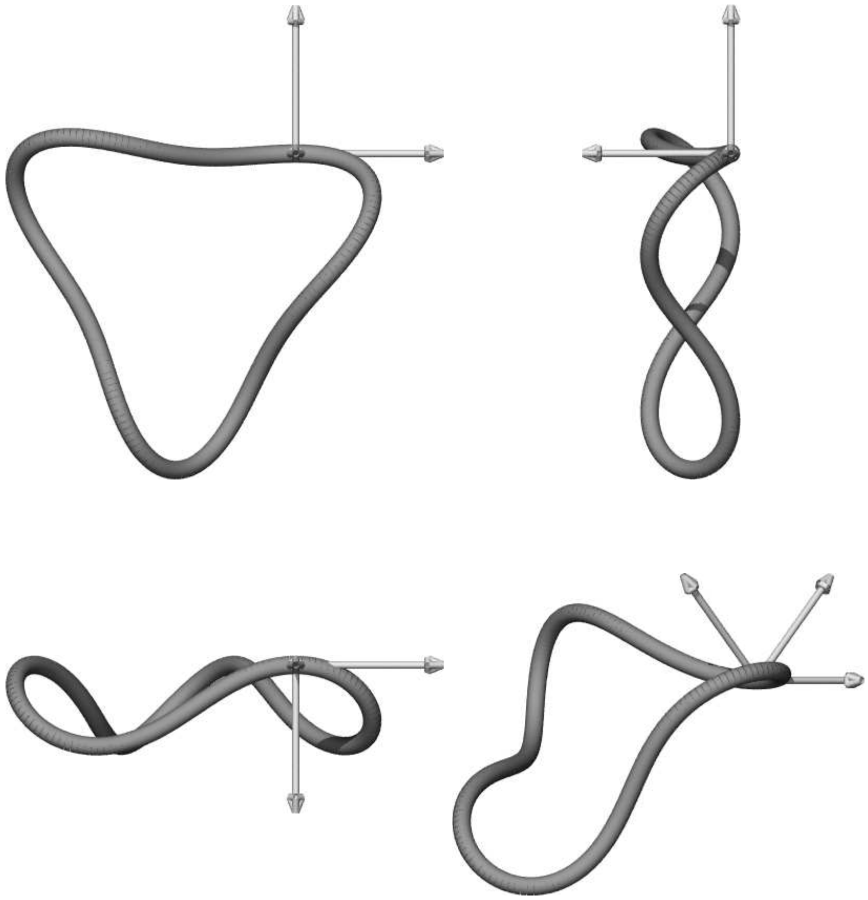

FIG. 5.3 *Figures 5.3, 5.4, and 5.5 show a sequence of three configurations on the branch linking the $(1, 2, -)$ bifurcation point to the $(2, 1, +)$ bifurcation point. Each figure depicts four views of the same equilibrium. All three configurations have period three symmetry in the plan view. The analogue of the self-intersecting figure-eight configuration is the self-intersecting trefoil shown in Figure 5.4. For twists slightly greater than the trefoil, the configuration becomes the non-intersecting trefoil knot shown in Figure 5.5, while the configuration shown in Figure 5.3 is unknotted.*

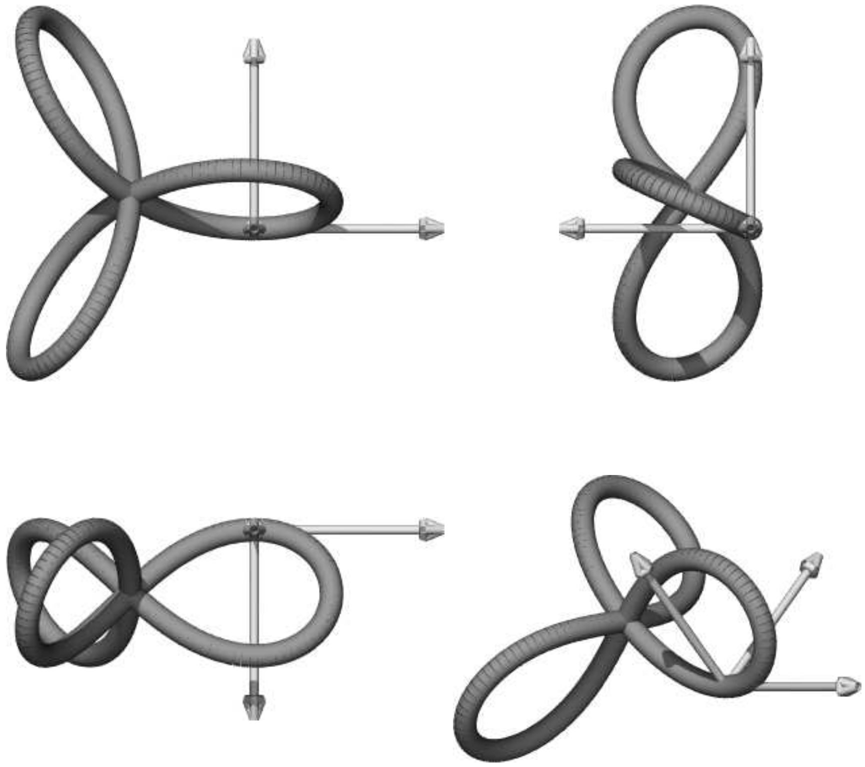

FIG. 5.4 *Figures 5.3, 5.4, and 5.5 show a sequence of three configurations on the branch linking the $(1, 2, -)$ bifurcation point to the $(2, 1, +)$ bifurcation point. Each figure depicts four views of the same equilibrium. All three configurations have period three symmetry in the plan view. The analogue of the self-intersecting figure-eight configuration is the self-intersecting trefoil shown in Figure 5.4. For twists slightly greater than the trefoil, the configuration becomes the non-intersecting trefoil knot shown in Figure 5.5, while the configuration shown in Figure 5.3 is unknotted.*

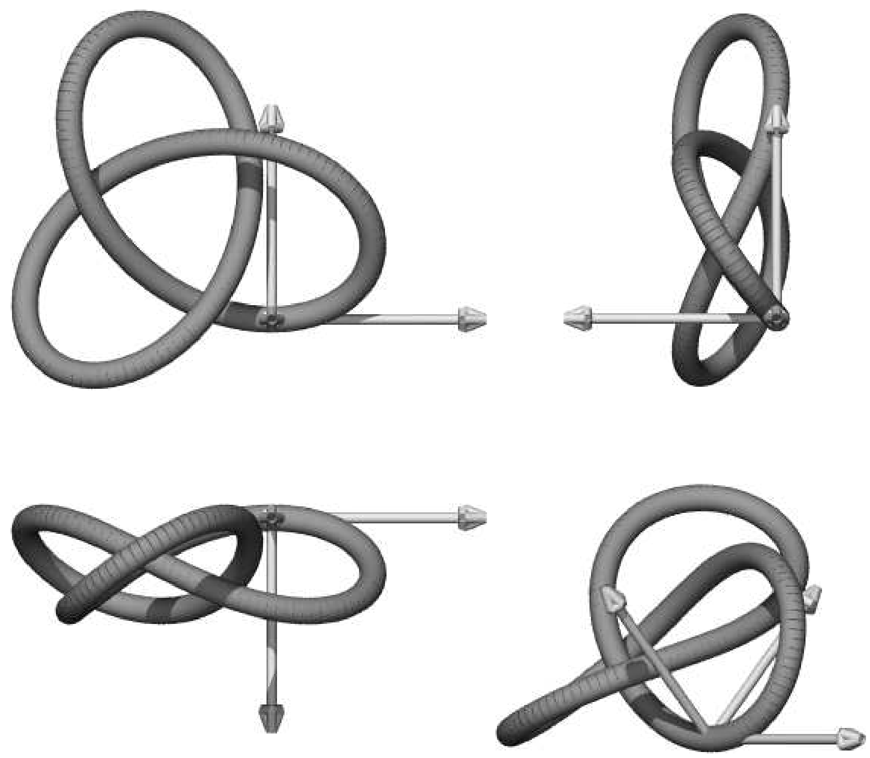

FIG. 5.5 *Figures 5.3, 5.4, and 5.5 show a sequence of three configurations on the branch linking the* $(1, 2, -)$ *bifurcation point to the* $(2, 1, +)$ *bifurcation point. Each figure depicts four views of the same equilibrium. All three configurations have period three symmetry in the plan view. The analogue of the self-intersecting figure-eight configuration is the self-intersecting trefoil shown in Figure 5.4. For twists slightly greater than the trefoil, the configuration becomes the non-intersecting trefoil knot shown in Figure 5.5, while the configuration shown in Figure 5.3 is unknotted.*

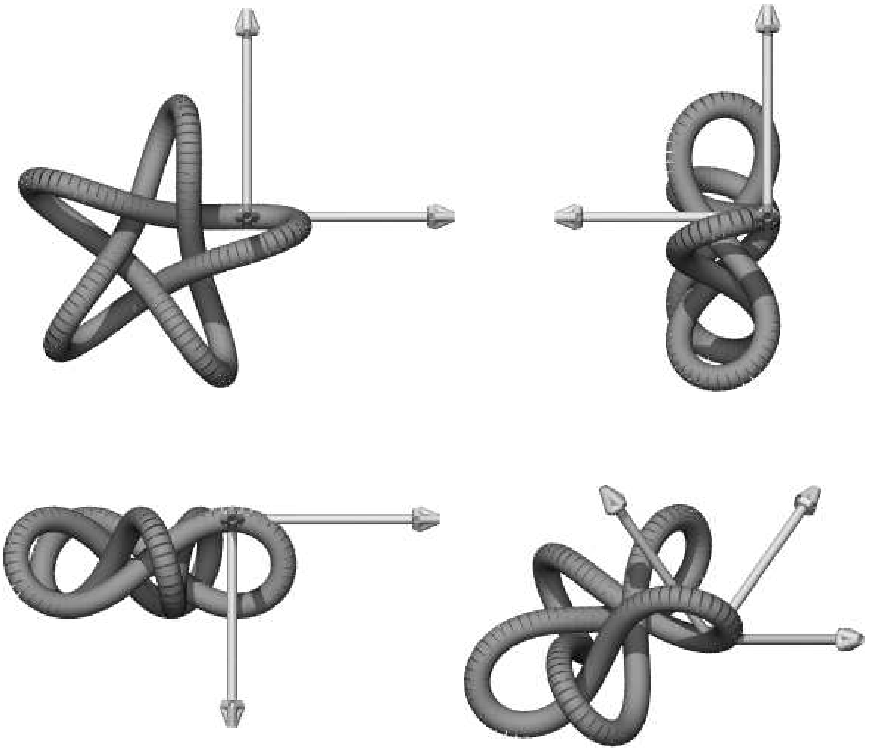

FIG. 5.6 *A knotted configuration on the* $(2, 3, +)$ *to* $(3, 2, -)$ *branch with five fold symmetry.*

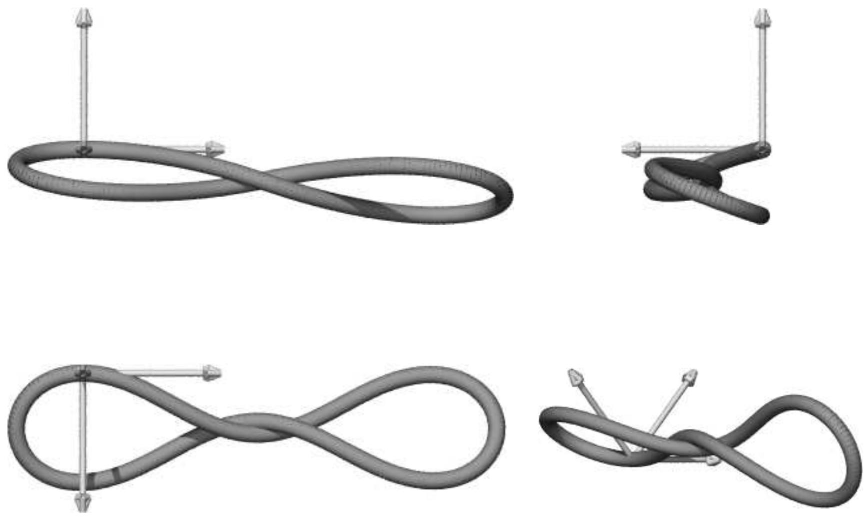

FIG. 5.7 *A configuration calculated with a modified code that models forces of self-contact which forbid self-intersection. Instead of passing through itself after self-contact at the figure eight solution, the rod starts to wrap around itself, forming the start of a plectoneme.*

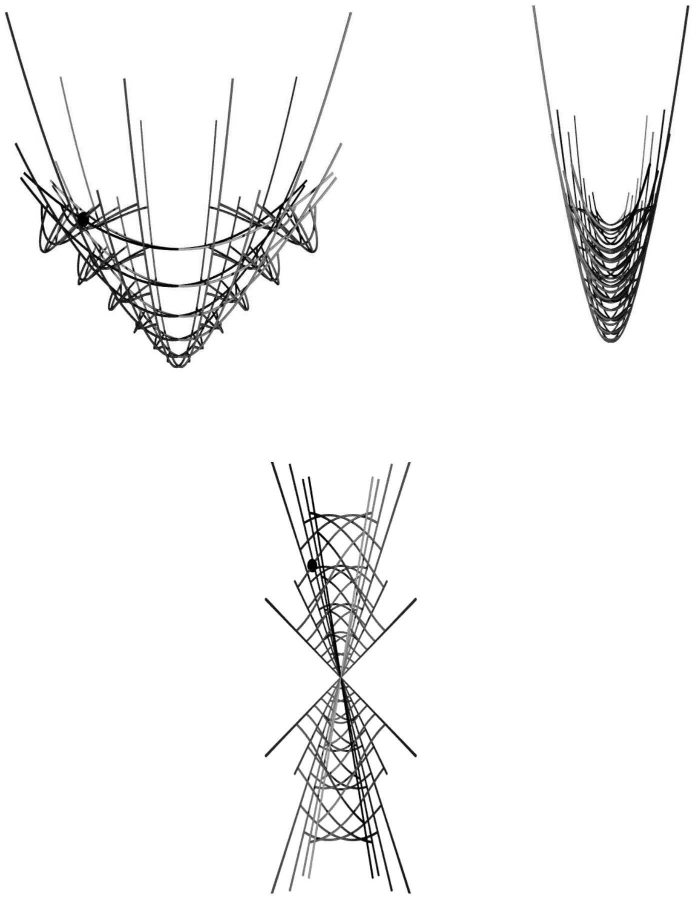

FIG. 5.8 *Three perspective views of the bifurcation diagram that arises when the energy, shear force, twist and writhe are evaluated along families of equilibria. The ordinate and abscissa in the top left, top right and bottom center views of the solution set are respectively energy vs. twist, twist vs. force, and energy vs. force. (The curves can also be colored according to writhe, but this information is lost in the greyscale presented here.) The 'trivial' circular solutions correspond to the straight branches in the bottom projection, and to the parabolic branches in the other two projections. The other solution branches correspond to configurations in which the centerline is a nonplanar curve. The nontrivial branches bifurcate from and link the trivial planar solutions according to the relation* $(M, N, +) \leftrightarrow (N, M, -)$. *All branches for* $(M + N) \leq 7$ *are shown.*

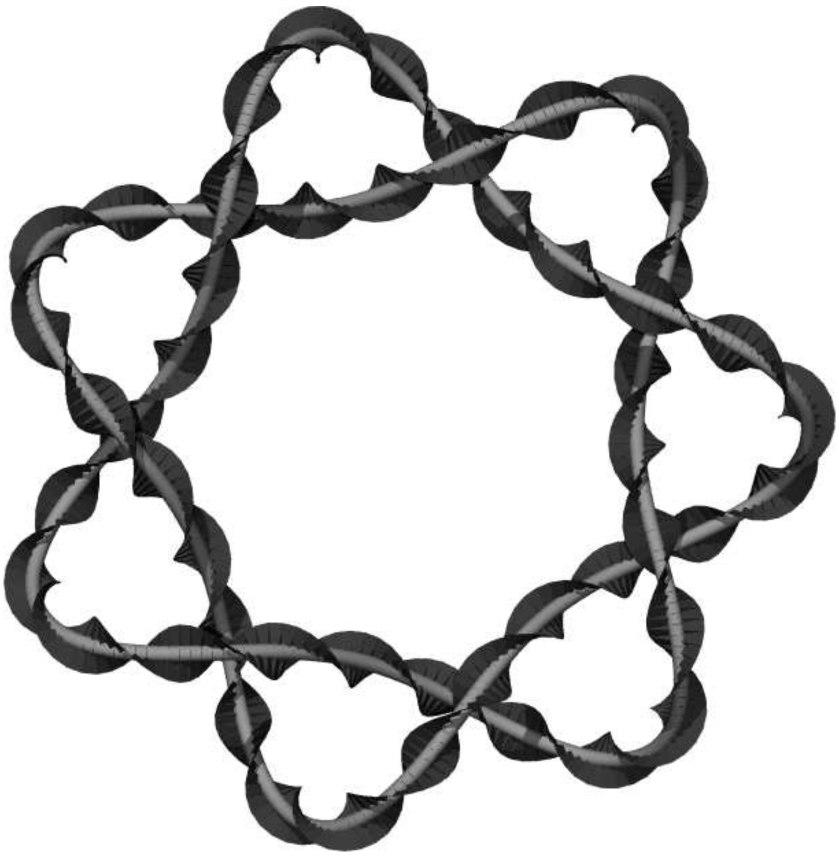

FIG. 5.9 *The reconstructed physical configuration corresponding to the point indicated by the filled circle in the bifurcation diagram of Figure 5.8. The cylinder represents the center line of the configuration, and the ribbon shows how the rod has been twisted. In the actual software package any point on the bifurcation diagram can be selected with a mouse click, and the physical solution is constructed and displayed in a second viewing window.*

Acknowledgements: It is a pleasure for the authors to thank the other members of the Numerical Analysis Laboratory in the Institute for Physical Sciences and Technology, and particularly Kathleen Rogers and Randy Paffenroth for their valuable contributions to this work.

REFERENCES

[1] Antman, S.S. **Nonlinear Problems of Elasticity**. (Springer-Verlag, New York, 1994).

[2] Bauer, W.R., R.A. Lund & J.H. White. Twist and Writhe of a DNA Loop Containing Intrinsic Bends. *Proc. Natl. Acad. Sci. USA* **90** (1990) 833-837.

[3] Beliaev, A. & A. Il'ichev. Conditional Stability of Solitary Waves Propagating in Elastic Rods. *Physica D* **90** (1996) 107.

[4] Benham, C.J. Onset of writhing in circular elastic polymers. *Phys. Rev. A* **39** (1989) 2582-2586.

[5] Bottema, O. & B. Roth. **Theoretical Mechanics** (Dover, New York, 1979).

[6] Caflisch, R.E. & J.H. Maddocks. Nonlinear dynamical theory of the elastica. *Proc. Roy. Soc. Edinburgh* **99A** (1984) 1-23.

[7] Coleman, B.D. & J-M. Xu. On the Interaction of Solitary Waves of Flexure in Elastic Rods. *Acta Mechanica* **110** (1995) 173-182.

[8] Dichmann, D.J. Hamiltonian Dynamics of an Elastica and Stability of Solitary Waves. Ph. D. thesis, University of Maryland (1994).

[9] Dichmann, D.J., J.H. Maddocks & R.L. Pego. Hamiltonian Dynamics of an Elastica. *Arch. Rational Mech. Anal.* forthcoming.

[10] Dichmann, D.J., J.H. Maddocks & J-M. Xu. Three-Dimensional Hamiltonian Dynamics of an Elastica and the Stability of Solitary Waves. In preparation.

[11] Dirac, P.A.M. On generalized Hamiltonian dynamics. *Can. J. Math.* **2** (1950) 129-148.

[12] Doedel, E. AUTO 86 User Manual. (Caltech, Dept. Applied Mathematics, Pasadena)

[13] Domokos, G. A group-theoretic approach to the geometry of elastic rings. *J. Nonlinear Science* **5** (1995) 453.

[14] Domokos, G. & R. Paffenroth. PCR - A Visualization Tool for Multi-Point Boundary Value Problems. Technical Note BN-1167. (University of Maryland, Institute for Physical Science and Technology, College Park, 1994).

[15] Falk, R.S. & J-M. Xu. Convergence of a Second-Order Scheme for the Nonlinear Dynamical Equations of Elastic Rods. *SIAM J. Numerical Analysis* **32** (1995).

[16] Goldstein, H. **Classical Mechanics**, Second Edition (Addison-Wesley, Reading, MA, 1981).

[17] Ilyukhin, A.A. **Spatial problems of non-linear theory of elastic rods**, (Naukova Dumka, Kiev, 1979). [in Russian]

[18] James, R.D. The equilibrium and post-buckling behaviour of an elastic curve governed by a non-convex energy. *J. Elasticity* **11** (1981) 239-269.

[19] Jülicher, F. Supercoiling transitions of closed DNA. *Phys. Rev. E* **49** (1994) 2429-2435.

[20] Kirchhoff, G.R. Ueber das Gleichgewicht und die Bewegung eines unendlich dünnen elastischen Stabes. **Gesammelte Abhandlungen** (Leipzig, 1882).

[21] Klapper, I. & M. Tabor. Dynamics of Twisted Elastic Rods. Preprint.

[22] Landau, L.D. & E.M. Lifshitz. **Theory of Elasticity** (Pergamon Press, New York, 1970).

[23] Langer, J. & D. Singer. Lagrangian Aspects of the Kirchhoff Elastic Rod. *SIAM Review* forthcoming

[24] LeBret, M. Catastrophic Variation of Twist and Writhing of Circular DNAs with Constraint? *Biopolymers* **18** (1979) 1709-1725.

[25] Li, Y. & J.H. Maddocks. On the Computation of Equilibria of Elastic Rods, Part I: Integrals, Symmetry and a Hamiltonian Formulation. Submitted to *J. Comp. Physics*

[26] Li, Y. & J.H. Maddocks. On the Computation of Equilibria of Elastic Rods, part II: Effects of Self-Contact. In preparation.

[27] Li, Y., J.H. Maddocks & D.J. Dichmann. On the Computation of Equilibria of Elastic Rods, part III: Effects of Shear. In preparation.

[28] Love, A.E.H. **A Treatise on the Mathematical Theory of Elasticity**, (Dover, New York, 1944).

[29] Maddocks, J.H. & D.J. Dichmann. Conservation Laws in the Dynamics of Rods. *J. Elasticity* **34** (1994) 83-96.

[30] Olver, P.J. **Applications of Lie Groups to Differential Equations**, (Springer-Verlag, New York, 1986).

[31] Shi, Y., A. Borovik & J.E. Hearst. Elastic Rod Model Incorporating Shear and Extension, Generalized Schrödinger Equations, and Novel Closed-Form Solutions for Supercoiled DNA. *J. Chem. Physics* **103** 3166 (1995)

[32] Shi, Y. & J.E. Hearst. The Kirchhoff elastic rod, the nonlinear Schrödinger equation, and DNA supercoiling. *J. Chem. Phys.* **101** (1994) 5186-5200.

[33] Schlick, T. Modeling Superhelical DNA: Recent Analytical and Dynamical Approaches. **Current Opinions in Structural Biology**, ed. B. Honig. **5** (1995).

[34] Schlick, T., W.K. Olson, T. Westcott & J.P. Greenberg. On Higher Buckling Transitions in Supercoiled DNA. *Biopolymers* **34** (1994) 565-597.

[35] Shuster, M.D. A Survey of Attitude Representations. *J. Astronautical Sciences* **41** (1994) 439-518.

[36] Simo, J.C., J.E. Marsden & P.S. Krishnaprasad. The Hamiltonian Structure of Nonlinear Elasticity: The Material and Convective Representations of Solids, Rods and Plates. *Arch. Rational Mech. Anal.* **104** (1988) 125-183.

[37] Simo, J.C. & L. Vu-Quoc. A Three-Dimensional Finite-Strain Rod Model. Part II: Computational Aspects. *Comput. Meths. Appl. Mech. Engrg.* **58** (1986) 79-116.

[38] Starotsin, E.L. Three-Dimensional Conformations of Looped DNA in an Elastomechanical Approximation. *Proc. 2nd International Conference on Nonlinear Mechanics*. Ed. Chien Wei-zang. (Peking University Press, Peking, 1993).

[39] Tsuru, H. Equilibrium Shapes and Vibrations of Thin Elastic Rods. *J. Phys. Soc. Japan* **56** (1987) 2309-2324.

[40] Wadati, M. & H. Tsuru. Elastic Model of Looped DNA. *Physica D* **21** (1986) 213-226.

[41] Yang, Y., I. Tobias & W.K. Olson. Finite Element Analysis of DNA Supercoiling. *J. Chem. Phys.* **98** (1993) 1673-1686.